

**WEAK INTERACTIONS OF QUARKS AND
LEPTONS: EXPERIMENTAL STATUS***

STANLEY WOJCICKI
Physics Department and
Stanford Linear Accelerator Center
Stanford University, Stanford, CA. 94305

Lectures presented at the
12th SLAC Summer Institute on Particle Physics
The Sixth Quark

Stanford, California
July 23 - August 3, 1984

* Work supported by the Department of Energy, contract numbers DE-AC03-76SF00515 and DE-AC03-ER40050, and The National Science Foundation.

© Stanley Wojcicki 1984

TABLE OF CONTENTS

1. Introduction	
2. The Quark Mixing Matrix	
3. CP Violation	
4. Rare Decays	
5. Status of the Lepton Sector	
6. Right-Handed Currents	

REFERENCES

1. Introduction

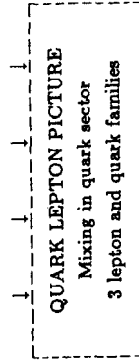
The work on the subject of weak interactions spans the last half a century. In assessing where we are today and where we might be going in the near future it is useful to look at the historical development of this field. Furthermore, we can say that the task of the high energy physicist is to understand the basic constituents of matter and of the forces that govern their behavior. Thus, in the spirit of the title of this talk, I start out by outlining the development¹⁾ of our present picture of the constituents and the present picture of the weak force which determines at least a part of their mutual interactions.

Figure 1 attempts schematically to outline the major milestones in the development of the picture we shall be discussing. There is undoubtedly certain arbitrariness in the choice of these milestones but hopefully they do represent reasonably fairly the logical development of the subject. In the "constituent sector" I take the discovery of the muon as the logical starting point since that was the first indication that the spectrum one is dealing with is richer than initial observations might have indicated. The unexpected discovery of strange particles followed by observation of the electron neutrino and the famous 2 neutrino experiment were other key steps in the initial elucidation of the quark-lepton picture.

The decade of the 1960s saw the birth of the quark concept and its subsequent growth to maturity. The initial spectroscopic measurements led to the quark postulate and culminated in the discovery of the predicted Ω^- particle. The dynamical reality of the quarks was demonstrated beautifully in a series of deep inelastic scattering experiments, first with electrons using the SLAC accelerator and subsequently with the neutrinos and muons, mainly at Fermilab and CERN. The decade of the 1970s brought us an enlargement of both the quark and lepton sectors with the observation of the postulated charm quark and the totally unexpected τ lepton. The subsequent measurements of the properties of these two new constituents confirmed the initial belief that they represent an

EVOLUTION OF THE CONSTITUENT PICTURE

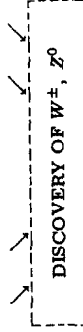
Discovery of the muon
 Discovery of strange particles
 Observation of ν_e
 $\nu_\mu - \nu_e$ experiment
 Hadron spectroscopy \rightarrow quark picture
 Ω^- discovery
 Dynamic evidence for quarks and gluons \rightarrow
 deep inelastic e, ν, μ scattering
 Charmonium and bare charm
 r and its properties
 QED experiments \rightarrow point nature of leptons
 T discovery
 b quark spectroscopy
 Discovery of the top quark



EVOLUTION OF OUR PICTURE OF WEAK FORCE

1950s
 Charged Currents
 Observation of ν_e
 Parity non-conservation
 V-A theory
 $\nu_\mu - \nu_e$ distinction
 Cabibbo theory
 Phenomenology of C.C.
 ν interactions

1970s
 Neutral Currents
 G.W.S. model
 Discovery of N.C.
 $\nu - e$ scattering
 $e^- d$ scattering (polarized)
 Interference effects in
 weak - e.m. interactions
 $(e^+ e^- \rightarrow \mu^+ \mu^-)$



1980s and beyond
 W.I. of High Mass Scales

Testing the standard model
 Searches for something new
 Violation of conservation laws
 Discrepancies
 New particles

Figure 1 A rough outline of the historical development of our present picture of quarks and leptons and their weak interactions.

addition to the family of the fundamental building blocks.

Finally the late 1970s and early 1980s provided us with evidence for, and properties of, the fifth quark. Just now we may be in the process of completing the quark sextet with the recent observations at CERN.

One should not neglect the important contributions to this picture from the many beautiful QED experiments demonstrating the point nature of the leptons, ranging from the ultra-high precision static experiments to the highest energy $e^+ e^-$ QED processes.

Thus we have arrived at our present picture of the three doublet families of quarks and three doublet families of leptons. In addition we have learned that the mass eigenstates and weak interaction eigenstates are different in the quark sector. The reasons for the similarities and differences in this quark-lepton picture are one of the key puzzles in high energy physics today.

We turn now to the evolution of our present understanding of the weak interactions. I find it natural to distinguish between two different topics associated with two different eras in the study of this field - the charged current sector with its golden age in the 1950s and the neutral current sector with the height of its development in the 1970s. The key nuclear physics experiments in the 1950s on the nature of the weak interaction, parity nonconservation, and neutrino helicity, coupled with the seminal theoretical ideas about parity violation and the conserved vector current hypothesis led to the establishment of the presently accepted V-A picture of charged current interactions. The experiments on decays of elementary particles and the program on neutrino interactions reinforced this picture and developed further the phenomenology of weak interactions.

Our understanding of neutral currents also progressed very rapidly with the height of activity in the late 1970s. A few years after the formulation of the Glashow-Weinberg-Salam model (GWS), neutral currents were discovered at CERN and their existence confirmed soon afterwards at Fermilab. There followed several important experiments culminating in the key polarized electron-deuteron

scattering asymmetry measurement at SLAC: The subsequent experimental work provided even more stringent tests, all of them reinforcing our belief in the validity of the GWS picture.

Both of those rather separate lines of investigation have culminated in the recent discoveries at CERN of the W and Z gauge bosons. This key experiment can be viewed as bringing to a successful end the previous 50 years of work on weak interactions. We can justifiably ask where do we go from here.

It is my opinion that the next decade will emphasize the weak interactions of higher mass scales. Thus we shall try to answer the questions that will address the existence and the properties of the postulated (as well as the unexpected) higher mass particles and their roles as mediators of the weak interactions. This physics will span a range of investigations including detailed tests of the standard model with the hope of discovery of small discrepancies as well as searches for totally new phenomena, whether these be violations of existing laws, new particles, or something totally unexpected. The techniques employed will undoubtedly be numerous, ranging from atomic and nuclear experiments, through proton decay, ν decay and oscillation searches and cosmic ray studies, to the experiments at the highest energies which will hopefully be opened up by the next generation of accelerators. Finally, it may also be hoped that these "high mass scale investigations" will at the same time shed light on the puzzles that are present today in the constituent sector.

The choice of topics adopted for these lectures can be understood in the context of the above discussion. My emphasis will be less on how we got here rather than on where we are and where we are going from here. Hence, I will discuss the present experimental status of weak interactions, with the emphasis on the problems and questions and on the possible lines of future investigations.

2. The Quark Mixing Matrix

In our present picture of the quark sector, we have three left-handed doublets:

$$\begin{pmatrix} u \\ d' \end{pmatrix}_L, \begin{pmatrix} c \\ s' \end{pmatrix}_L, \text{ and } \begin{pmatrix} t \\ b' \end{pmatrix}_L$$

It is furthermore known experimentally that the quark mass eigenstates (denoted by the unprimed symbols) are not the same as the quark gauge group eigenstates (denoted by primed symbols). There is a certain arbitrariness in parametrizing this fact. The convention is to define the phases in such a way that the two sets of eigenstates are identical for the $q = 2/3$ quark states i.e., $u = u', c = c'$, and $t = t'$. We can then define a unitary matrix, U, which is totally specified by four real parameters conventionally taken to be three angles and one phase. This matrix can then be thought of as giving us the relationship between the (d', s', b') states and the (d, s, b) states i.e., schematically

$$q' = Uq \quad (2.1)$$

Alternatively, the matrix U can be said to specify the quark couplings in the charge-changing weak interaction current, i.e.

$$J^\mu = \bar{q}^+ \gamma^\mu (1 - \gamma_5) U q^- \quad (2.2)$$

with the $q^+(q^-)$ symbols standing for the positive (negative) charge quark states.

The matrix U is similar to the Euler matrix representing a rotation in the three-dimensional space. There are several parametrizations of this matrix. The original one, due to Kobayashi and Maskawa,²⁾ is

$$\begin{pmatrix} C_1 & -S_1 C_3 & -S_1 S_3 \\ S_1 C_2 & C_1 C_2 C_3 - S_2 S_3 e^{i\delta} & C_1 C_2 S_3 + S_2 C_3 e^{i\delta} \\ S_1 S_2 & C_1 S_2 C_3 + C_2 S_3 e^{i\delta} & C_1 S_2 S_3 - C_2 C_3 e^{i\delta} \end{pmatrix}$$

where $C_i \equiv \cos\theta_i$, $S_i \equiv \sin\theta_i$; $i = 1, 2, 3$ and $\theta_1, \theta_2, \theta_3$ are three angles equivalent to Euler angles and δ is the phase mentioned above. It was the contribution of

Kobayashi and Maskawa to point out that the CP violation can be introduced naturally if one has 6 quarks (rather than 4 known at that time) and provided that the phase $\delta \neq 0$ or π .

The other representation that finds frequent use is due to Maiani³⁾ and is given by

$$\begin{pmatrix} C_\beta C_\theta & C_\beta S_\theta & S_\beta \\ -S_\gamma C_\theta S_\beta e^{i\delta} - S_\theta C_\gamma & C_\gamma C_\theta - S_\gamma S_\beta S_\theta e^{i\delta} & S_\gamma C_\beta e^{i\delta} \\ -S_\beta C_\gamma C_\theta + S_\gamma S_\theta e^{i\delta} & -C_\gamma S_\beta S_\theta - S_\gamma C_\theta e^{-i\delta} & C_\gamma C_\beta \end{pmatrix}$$

where $C_\theta \equiv \cos\theta$, $S_\theta \equiv \sin\theta$, etc.

Even within the framework of each representation there are several different phase conventions that are used in the literature. These do not present a problem for us since the experiments that we shall discuss determine only the absolute magnitude of each particular matrix element. Finally, we should remark that one can define each angle to be in the first quadrant. The phase δ can then range from 0 to 2π and must be determined by experiment.

There are certain advantages to each representation. In the original K-M representation all the angles, $\theta_1, \theta_2, \theta_3$ are relatively small and thus the form of the matrix explicitly shows that the U_{13} element, for example, is second order in these small quantities. In the Maiani representation, θ, β , and γ are also small, and in that approximation the matrix becomes simply

$$\begin{pmatrix} 1 & \theta & \beta \\ -\theta & 1 & \gamma \\ -\beta & -\gamma & 1 \end{pmatrix}.$$

Thus the angles θ, β, γ are approximately related to the size of the amplitude describing the couplings $u \rightarrow s$, $u \rightarrow b$, and $c \rightarrow b$ respectively.

A third parametrization of the mixing matrix has been recently introduced by Wolfenstein.⁴⁾ That particular parametrization is convenient for the analysis

of the CP problem insofar that it explicitly shows that the CP violation enters only multiplied by a third power of a small parameter λ .

Our procedure in this discussion will be to describe the experimental input that allows us to measure the general matrix elements, i.e.,

$$\begin{pmatrix} U_{ud} & U_{us} & U_{ub} \\ U_{cd} & U_{cs} & U_{cb} \\ U_{td} & U_{ts} & U_{tb} \end{pmatrix}.$$

At the end we shall try to relate that experimental input to the values of the K-M representation parameters $\theta_1, \theta_2, \theta_3$ and δ .

Before embarking on this task, it might be worthwhile to summarize the phenomenological need for the top quark that would complete the third doublet. In other words, the question that one asks is whether the experimental data is compatible with the b quark being a singlet. This question might be moot in light of the recent evidence⁵⁾ for a possible new quark state from CERN, but until these data are shown to be completely conclusive, it is worthwhile to keep an open mind on this point.

A rather general argument on this point has been recently presented by Kane and Peskin⁶⁾ and we reproduce here its general qualitative features. The authors show that in any model in which the b quark is an $SU(2)$ singlet with conventional W^\pm and Z^0 couplings the following inequality involving semileptonic decays has to be satisfied:

$$\frac{\Gamma(B \rightarrow X\ell^+\ell^-)}{\Gamma(B \rightarrow X\ell^+\nu)} \geq 0.12 \quad (2.3)$$

where ℓ^\pm is the generic symbol for charged leptons. Furthermore, the alternative models, which do not make this standard coupling assumption, are either already ruled out by the data or extremely unattractive.

The essence of the argument is as follows. The b quark is known to decay and thus must decay by virtue of mixing. The two weak eigenstates representing

$q = -1/3$ quark states can then be written as:

$$d' = \sum_{i=1}^3 \alpha_i q_i \quad \text{and} \quad (2.4)$$

$$s' = \sum_{i=1}^3 \beta_i q_i$$

where α_i , β_i are mixing coefficients and $q_i = d, s$, or b . In Fig. 2 we show the diagrams that must be responsible for leptonic decays of the b quark. As can be seen from these diagrams the decay rates are given solely by the couplings of the gauge bosons to the leptons and to the quarks. The former are determined entirely in the framework of the Glashow-Weinberg-Salam model⁷⁾; the latter are given by the model if the mixing coefficients (α 's and β 's) are known. Accordingly, the problem reduces to finding these coefficients which minimize the ratio given in 2.3 and at the same time are compatible with the other experimental data. To put it in other words the Glashow-Weinberg⁸⁾ theorem which shows that the GIM mechanism for suppression of neutral currents is applicable for any number of weak doublets, is no longer relevant if b quark is a weak singlet. Hence, the mixing coefficients have to be adjusted "by hand" so as to minimize the flavor changing neutral current amplitude in b decay and to make those amplitudes in other decays compatible with the very stringent experimental limits.

One makes now the observation that the mixing angles are rather well constrained already by the existing data. Specifically if the first equation in 2.4 is rewritten as

$$d' = C_1(C_c d + S_c s) + S_1 b,$$

C_1 is constrained to be very close to 1 by Cabibbo universality and S_c is the sine of the Cabibbo angle that is well measured in K and hyperon decays. Additional constraints are imposed by the requirements of orthogonality of s' and d' and the requirement that the strangeness changing $d \leftrightarrow s$ neutral current amplitude be small enough to be compatible with the $K_L - K_S$ mass difference. The net effect

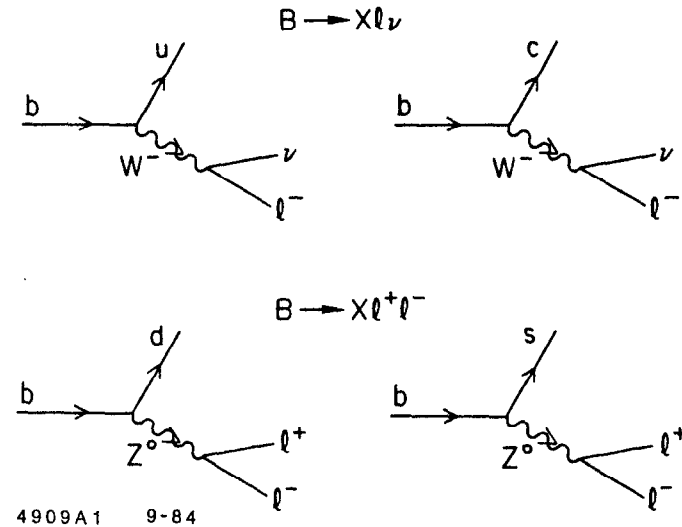


Figure 2 Diagrams contributing to semileptonic b decay.

of these constraints is that the mixing parameters are strongly constrained and the lower bound stated in 2.3 is obtained.

The best experimental limit comes from the data taken by the CLEO collaboration which obtains⁹⁾

$$\frac{B \rightarrow X\ell^+\ell^-}{B \rightarrow A\ell\ell} < 0.3\% \text{ (90\% C.L)} \quad (2.5)$$

Coupled with the world average⁹⁾ for each (i.e. electron and muon) semileptonic branching ratio of the B meson of $11.6 \pm 0.5\%$, this yields

$$\frac{\Gamma(B \rightarrow X\ell^+\ell^-)}{\Gamma(B \rightarrow X\ell^+\nu)} < 1.3\% \quad (2.6)$$

Thus the experimental value is clearly in contradiction with the Kane-Peskin bounds and excludes the b singlet possibilities. We next proceed to the discussion of the experimental determination of six out of the nine total elements U_{ij} .¹⁰⁾

a) U_{ud} responsible for $u \rightarrow d$ and $d \rightarrow u$ transitions.

We determine this matrix element by comparing the strength of nuclear vector beta decays to muon decay rate. To assure pure vector, i.e., Fermi transitions we have to limit ourselves to $0^+ \rightarrow 0^+$ decays. In addition, it is important that the nuclear matrix element be perfectly understood, which in turn implies use of superallowed transitions.

Several transitions satisfying these requirements exist in nature and have been studied experimentally. They generally are decays within the same $T = 1$ multiplet and the two that provide the most accurate information are ^{14}O and $^{26}\text{Al}^m$ decays. The data on those and other decays, satisfying the criteria outlined above, are presented in Table I below (reproduced from Paschos and Turke¹¹⁾).

Table I

ft-values, corrections and corresponding results for more accurate decays.

Nucleus	ft(s)	$\delta_R(\%)$	$\delta_C(\%)$	$\delta_W(\%)$	$ U_{ud} $
^{14}O	3047.6 ± 3.6	1.57	0.18	2.10	0.97223
$^{26}\text{Al}^m$	3037.9 ± 2.9	1.61	0.24	2.10	0.97377
^{34}Cl	3052 ± 12	1.68	0.51	2.10	0.97255
$^{38}\text{K}^m$	3063 ± 10	1.74	0.44	2.10	0.97015
^{42}Sc	3052 ± 13	1.81	0.44	2.10	0.97154
^{46}V	3039 ± 16	1.87	0.40	2.10	0.97311
^{50}Mn	3038.1 ± 7.1	1.95	0.47	2.10	0.97322
^{54}Co	3041.4 ± 5.0	2.01	0.56	2.10	0.97289

The relevant corrections are: δ_R , the "outer" electromagnetic correction, δ_C - the nuclear isospin correction to correct for isospin impurity in the transitions in question, and δ_W - the difference in "inner" electroweak correction between the nuclear ft values and the muon decay rate.

Paschos and Turke obtain from their analysis

$$U_{ud} = 0.9730 \pm 0.0004 \pm 0.0020$$

where the first error is statistical and the second represents theoretical uncertainties. An independent analysis by Shrock and Wang¹²⁾ using compilations by Towner and Hardy and by Wilkinson¹³⁾ as the basic input yields

$$U_{ud} = 0.9737 \pm 0.0025$$

Clearly these numbers are compatible with each other. As the best value I shall

take the average of the two, obtaining

$$U_{ud} = 0.9733 \pm 0.0024. \quad (2.7)$$

b) U_{us} responsible for $u \rightarrow s$ and $s \rightarrow u$ transitions.

There are two alternative approaches to measuring this matrix element and we shall discuss each one in turn.

1 - Analysis of the Ke_3 decays, i.e., of the processes

$$\begin{aligned} K^+ &\rightarrow \pi^0 e^+ \nu & \text{and} \\ K_L^0 &\rightarrow \pi^\pm e^\mp \nu \end{aligned}$$

There are several theoretical difficulties that have to be kept in mind when discussing these decay modes. First, we might expect some SU_3 breaking effects, even though they should be small here by virtue of the Ademollo-Gatto theorem.¹⁴⁾ Second, the momentum transfer involved is no longer negligible as in the case of the nuclear beta decay; hence the form factor behavior must be understood insofar as it is the rate at $q^2 = 0$ that is directly related to U_{us}^2 .

Experimentally, the input consists of the lifetimes of the two K mesons, the branching ratio into the $\pi e \nu$ mode and the form factor dependence allowing the extrapolation to obtain $f_+(0)$.

Shrock and Wang¹²⁾ apply radiative and SU_3 breaking corrections to the data to obtain

$$\begin{aligned} U_{us} &= 0.221 \pm 0.003 & \text{from } K^+ \text{ decays} & \text{and} \\ U_{us} &= 0.212 \pm 0.005 & \text{from } K_L^0 \text{ decays.} \end{aligned}$$

Combining these we obtain

$$U_{us} = 0.219 \pm 0.003. \quad (2.8)$$

2 - The other method consists of analysis of the combined hyperon and neutron decay rates. We first briefly describe qualitatively the formalism that is used

in this analysis. The general matrix element for hyperon (or neutron) decay can be expressed in terms of 6 form factors, three of which: f_1 , f_2 , f_3 are vector form factors and the other three, g_1 , g_2 , g_3 axial form factors. Only f_1 and g_1 , and to much lesser extent f_2 , give significant contribution to the experimentally observable quantities.

The amplitude of the strangeness conserving decays is proportional to U_{ud} ($\cos\theta$ in the old 4 quark formalism); of the strangeness changing decays to U_{us} ($\sin\theta$ in the 4 quark formalism). Furthermore, both f_1 and f_2 are determined entirely by the CVC hypothesis. The g_1 form factor for each decay is expressible as a linear combination of 2 parameters, F and D, which represent the strength of the symmetric and anti-symmetric $8 \otimes 8$ couplings. The exact parametrization of these 3 form factors is specified in Table II.

Table II
Parameters of the baryon weak matrix

Decay	Amplitude	$f_1(0)$	$f_2(0)^a$	$g_1(0)$
$n \rightarrow pe\nu_e$	$\cos\theta$	1	$\mu_p - \mu_n$	$F + D$
$\Sigma^\pm \rightarrow \Lambda e\nu_e$	$\cos\theta$	0	$-\sqrt{3/2}\mu_n$	$\sqrt{2/3}D$
$\Sigma^- \rightarrow \Sigma^0 e\nu_e$	$\cos\theta$	$\sqrt{2}$	$\sqrt{2}[\mu_p + (\mu_n/2)]$	$\sqrt{2}F$
$\Lambda \rightarrow pe\nu_e$	$\sin\theta$	$-\sqrt{3/2}$	$-\sqrt{3/2}\mu_p$	$-\sqrt{3/2}(F+D/3)$
$\Sigma^- \rightarrow ne\nu_e$	$\sin\theta$	-1	$-(\mu_p + 2\mu_n)$	$-(F - D)$
$\Xi^- \rightarrow \Lambda e\nu_e$	$\sin\theta$	$\sqrt{3/2}$	$\sqrt{3/2}(\mu_p + \mu_n)$	$\sqrt{3/2}(F - D/3)$
$\Xi^- \rightarrow \Sigma^0 e\nu_e$	$\sin\theta$	$1/\sqrt{2}$	$1/\sqrt{2}(\mu_p - \mu_n)$	$(F+D)/\sqrt{2}$
$\Xi^0 \rightarrow \Sigma^+ e\nu_e$	$\sin\theta$	1	$\mu_p - \mu_n$	$F+D$
$\Xi^- \rightarrow \Xi^0 e\nu_e$	$\cos\theta$	1	$\mu_p + 2\mu_n$	$F - D$

^a The values of the anomalous magnetic moments are: $\mu_p = 1.793$, $\mu_n = -1.913$.

Every measurable in these decay processes (decay rates, asymmetry parameters, angular correlation coefficients) can be expressed in terms of the form factors discussed above. Thus once $\sin\theta$ (and hence $\cos\theta$) is known, each independent piece of data determines a straight line in the D, F space. Hence the analysis can be thought of as consisting of finding that value of $\sin\theta$ which results in all of those straight lines intersecting in a common point, or more specifically, minimizing the "circle of least confusion."

The latest experimental results from the hyperon decay experiment at CERN¹⁵⁾ are displayed in Fig. 3. In addition, data on neutron lifetime and neutron decay angular correlations are also shown on the same figure. There is some controversy and inconsistency in the neutron lifetime data. For the purpose of this plot a value of $\tau_n = 925.3 \pm 11.1$ sec has been used by the authors of Ref. 15. The lines labeled (g_1/f_1) represent the angular correlation measurements; the other lines come from the partial rate measurements. The shaded area represents the extent of the experimental errors. Clearly the data are quite consistent and a least squares fit yields for the best values of the parameters:

$$\begin{aligned} F &= 0.477 \pm 0.012, \\ D &= 0.756 \pm 0.011, \quad \text{and} \\ \sin\theta \equiv U_{us} &= 0.231 \pm 0.003. \end{aligned}$$

This value of U_{us} is somewhat different from the K decay value ($\sim 3\sigma$). This probably reflects the theoretical uncertainties in both analyses. Accordingly, it is probably best to take the average value and increase the error somewhat to take into account these uncertainties. Thus we quote

$$U_{us} = 0.225 \pm 0.005. \quad (2.9)$$

Before leaving this topic, one should mention that there exists one set of data that is inconsistent with the above picture, namely the measurements of the α_+ ,

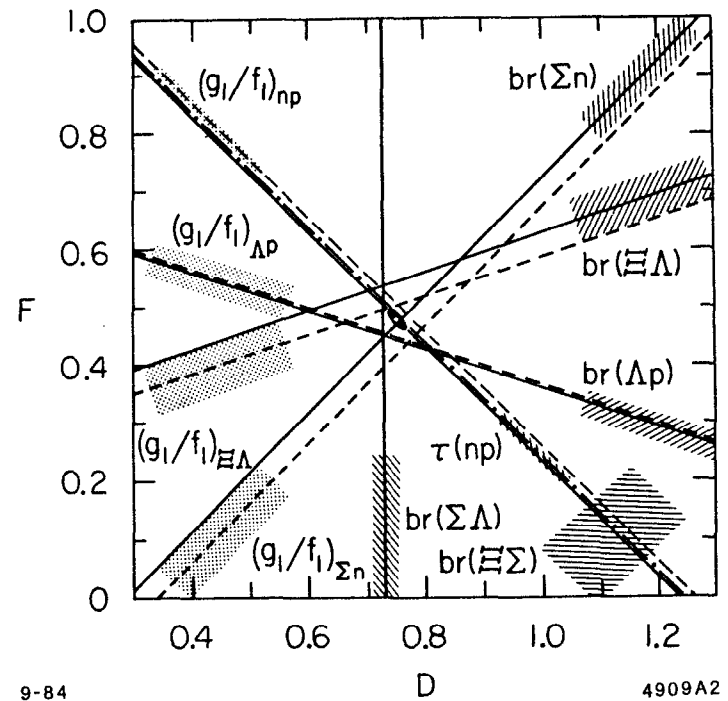


Figure 3 Summary of the hyperon decay data (from CERN experiment) and the neutron decay rate.

the decay asymmetry parameter for Σ^- . These data are illustrated in Fig. 4, together with the prediction from the overall fit to the CERN data. The present consensus is to discount this disagreement somewhat, since all these data points come from low statistics experiments, done in less than optimum conditions. There is an experiment¹⁶⁾ at Fermilab, which just completed its data-taking phase, which uses a polarized Σ^- beam and attempts to reconstruct the full Σ^- decay by measuring both the decay neutron and the decay electron. The results from that experiment should definitely settle this particular question.

c) U_{cd} responsible for $c \rightarrow d$ and $d \rightarrow c$ transitions.

In principle, there are two ways of extracting this parameter out of the data and we shall discuss each one in turn.

1 - We can study the $c \rightarrow d$ transitions in the charm decays. The ideal processes would be the decays

$$D \rightarrow \pi l \nu \quad \text{and} \\ D \rightarrow \rho l \nu$$

since these are unencumbered by the effects of strong interactions in the final state.

In practice neither of these decay modes has been observed as yet. Even when some data on these channels will be accumulated, there will still be certain conceptual difficulties with the proper analysis e.g., SU_4 breaking effects, mass of the charm quark to be used and form factor dependance. The pure hadronic decays $D \rightarrow 2\pi$ and $D \rightarrow K^+K^-$ have been observed but the extraction of U_{cd} out of these data does not appear to be possible at the present time. The fundamental difficulty lies in the fact that the hadronic effects simply are not understood well enough theoretically to be able to extract quantitative results. To illustrate this fact we remind the reader that experimentally¹⁷⁾

$$\frac{\Gamma(D^0 \rightarrow K^+K^-)}{\Gamma(D^0 \rightarrow \pi^+\pi^-)} \approx 3.5$$

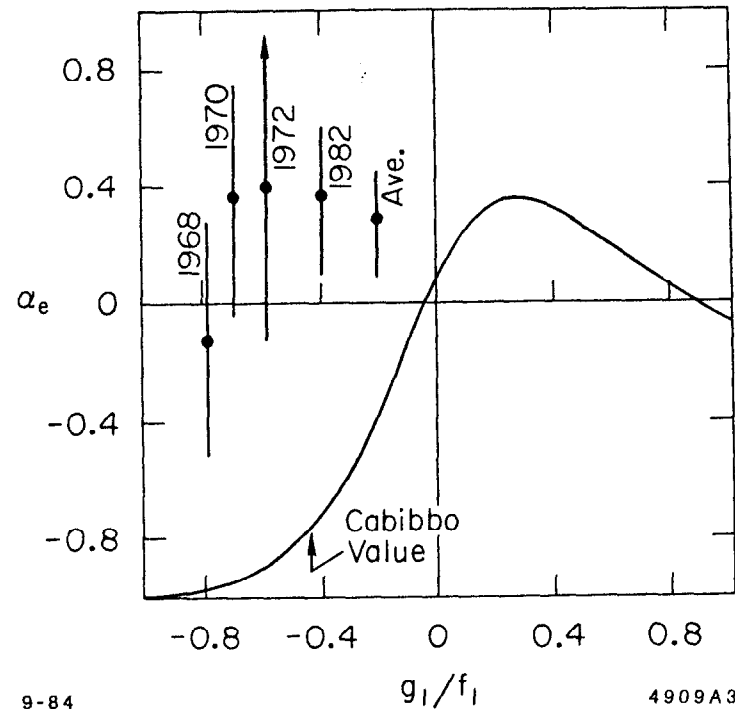


Figure 4 The four measurements of the Σ^- asymmetry parameter (α_e) compared with the prediction of the overall fit. The curve shows the dependance of the α_e on the ratio of form factors (g_1/f_1).

whereas the phase space effects would tend to favor the $\pi^+\pi^-$ mode. To my knowledge, no satisfactory explanation of this discrepancy has been given.

In addition there is the experimental fact that the lifetimes of D^0 and D^+ do not appear to be equal. Specifically using Hitlin's compilation¹⁸⁾ we have

$$\tau^+/\tau^0 = 2.78 \begin{matrix} +0.86 + 0.31 \\ -0.60 - 0.42 \end{matrix}$$

This can be understood at least qualitatively on the basis of the fact that the exchange diagrams that contribute to the D^0 decay are absent in the case of the D^+ decay (see Fig. 5). However, I am not aware of any reliable theoretical calculations that are able to reproduce accurately this number.

Thus at best we can conclude from the non-leptonic decay modes that the $c \rightarrow d$ transition is suppressed with respect to the $c \rightarrow s$ rate. Extraction of any quantitative information out of the charm Cabibbo forbidden decays, however, will have to await better experimental data or better theoretical understanding or both.

2 - Quantitative information on the U_{cd} matrix element can be obtained from the charm production by neutrinos. More specifically, one studies a $\mu^+\mu^-$ final state that is dominated by the sequence

$$\begin{aligned} \nu + p \text{ (or } n) &\rightarrow \text{charm} + \mu^- \\ &\quad \downarrow \\ &\quad \mu^+ + X \end{aligned}$$

which on the quark level can be written as

$$\begin{aligned} \nu + d &\rightarrow \mu^- + c \\ &\quad \downarrow \\ &\quad s + \mu^+ + \nu \end{aligned}$$

or

$$\begin{aligned} \nu + s &\rightarrow \mu^- + c \\ &\quad \downarrow \\ &\quad s + \mu^+ + \nu \end{aligned}$$

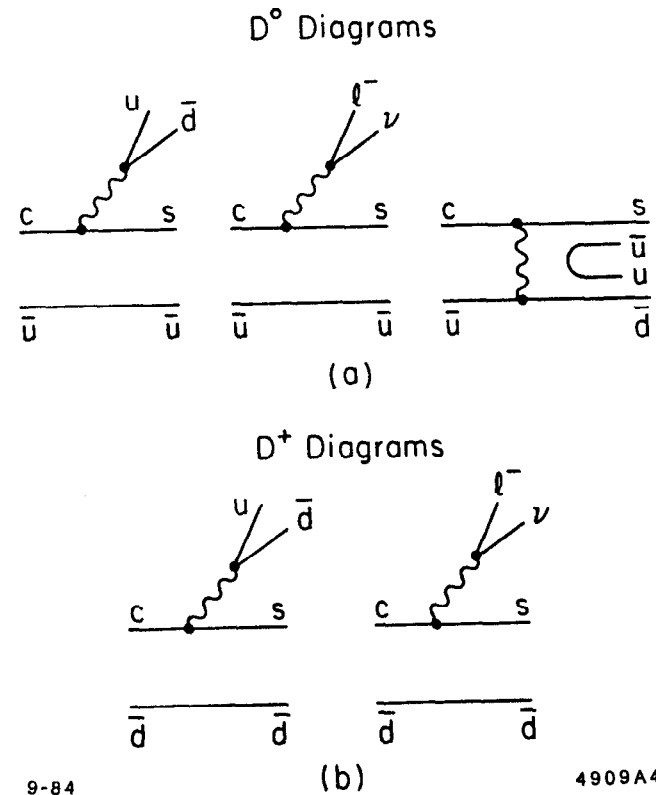


Figure 5 The standard diagrams that contribute to D^0 (a) and D^+ (b) decay (Cabibbo allowed).

and comparable reaction for the incident ν 's.

To obtain the value of U_{cd} we must separate the two quark contributions. The expressions for differential charm production cross sections by neutrinos and anti-neutrinos on an isoscalar target (a good approximation for heavy target experiments) are given by:

$$\frac{d^2\sigma^\nu}{dx dy} = \frac{G^2 M E_\nu x}{\pi} \{ |U_{cd}|^2 [u(x) + d(x)] + |U_{cs}|^2 \cdot 2s(x) \}, \quad (2.10)$$

$$\frac{d^2\sigma^{\bar{\nu}}}{dx dy} = \frac{G^2 M E_{\bar{\nu}} x}{\pi} \{ |U_{cd}|^2 [\bar{u}(x) + \bar{d}(x)] + |U_{cs}|^2 \cdot 2\bar{s}(x) \} \quad (2.11)$$

where $u(x)$ and $d(x)$ are the u and d quark distributions in the proton and we have utilized the fact that $u(x)$ in proton is the same as $d(x)$ in neutron.

Experimentally, the best measurement is of the $2\mu/1\mu$ ratios i.e. of $\sigma_{+-}^p/\sigma_{-+}^p$ and of the $\sigma_{+-}^p/\sigma_{+}^p$. We note that for single muon production we have

$$\frac{d^2\sigma^\nu}{dx dy} \propto q(x) + (1-y)^2 \bar{q}(x), \quad (2.12)$$

$$\frac{d^2\sigma^{\bar{\nu}}}{dx dy} \propto \bar{q}(x) + (1-y)^2 q(x) \quad (2.13)$$

where $q(x)$ stands for $u(x)$, $d(x)$, and $s(x)$ and similarly for $\bar{q}(x)$. We can now define

$$R = \sigma_{+-}^p/\sigma_{-+}^p \quad (2.14)$$

and integrate the expressions 2.10 - 2.13. Using the fact that $s(x) = \bar{s}(x)$, after some algebra we obtain

$$B|U_{cd}|^2 = \frac{(\sigma_{+-}^p/\sigma_{-+}^p) - (R\sigma_{+-}^p/\sigma_{+}^p) \frac{2}{3}}{1-R}, \quad (2.15)$$

with B being the weighted average semileptonic branching ratio of the charmed particles, the weighting being determined by the relative production cross section of various charm particles in $\nu(\bar{\nu})$ interactions and the relative muon detection efficiency for those decay modes.

The detailed analysis of this reaction has been performed¹⁹⁾ by the CDHS group who used $R = 0.48 \pm 0.02$ and $B = 7.1 \pm 1.3\%$, the latter value obtained by studying relative charmed particle production in emulsions. The dimuon to single-muon cross section ratios used came from the CDHS experiment. For the value of $|U_{cd}|$ the authors obtain

$$|U_{cd}| = 0.24 \pm 0.03 \quad (2.16)$$

The CCFRR collaboration at Fermilab obtains a similar value²⁰⁾ (0.25 ± 0.07) from the analysis of their $\mu^+\mu^-$ data.

d) U_{cs} responsible for the $c \rightarrow s$ and $s \rightarrow c$ transitions.

Again, information here can be obtained both from the charm decays and from the charm production by neutrinos.

1 - The optimum charm decay channel to use is the process

$$D \rightarrow \bar{K} \ell^+ \nu$$

since this decay combines the best experimental input and fewest theoretical uncertainties. Nevertheless some problems remain and they tend to limit the accuracy with which we can measure this matrix element.

On the theoretical side we need to cope now with the potential SU_4 breaking effects which could be larger here than in the case of K decays. The form factor dependance could also be more important here since q^2 involved can be quite large. At present, there is no information on the Dalitz plot density for this decay. Finally the relationship of the decay rate to the value of $|U_{cs}|^2$ depends on the masses of the c and s quarks used.

Experimentally, for a specific decay, for example:

$$D^+ \rightarrow \bar{K}^0 e^+ \nu_e$$

we need to know the D^+ lifetime, exclusive branching ratio $D^+ \rightarrow e^+ X$, and the fraction of that exclusive mode that goes to $\bar{K}^0 e^+ \nu_e$. The difficulty in extracting

the rate of interest lies in the fact that τ_D^+ and τ_D^0 appear to be different and thus their leptonic branching ratios will not be equal. Most of the exclusive $D \rightarrow eX$ branching ratio measurements came from high energy e^+e^- annihilations, where the precise D^0/D^\pm production rate is not known very well experimentally.

The numbers we shall use are:

$$\begin{aligned} \tau_+/\tau_- &= 2.78 && \text{(Ref.18),} \\ \tau_D^+ &= (8.3 \pm 1.0) \times 10^{-13} \text{sec} && \text{(Ref.21),} \\ B(D \rightarrow eX) &= (8.4 \pm 0.6)\% && \text{(Ref.21),} \\ \sigma(D^0)/\sigma(D^+) &= 2.3 \pm 1.2 && \text{(Ref.22) and} \\ \Gamma(D \rightarrow Ke\nu)/\Gamma(D \rightarrow eX) &= 0.55 \pm 0.14 && \text{(Ref.23).} \end{aligned}$$

These values give

$$\begin{aligned} B(D^+ \rightarrow e^+X) &= (15 \pm 3)\% , \\ B(D^+ \rightarrow \bar{K}^0 e^+ \nu_e) &= (8 \pm 3)\% , \\ \text{and } \Gamma(D^+ \rightarrow \bar{K}^0 e^+ \nu_e) &= (1.0 \pm 0.3) \times 10^{11} \text{sec}^{-1} . \end{aligned}$$

Finally, to relate the last value to $|U_{cs}|$ we use²⁴⁾

$$\Gamma(D^+ \rightarrow \bar{K}^0 e^+ \nu_e) = 1.5 \times 10^{11} \text{sec}^{-1} \times |f_+^{D \rightarrow K}(0)|^2 \times |U_{cs}|^2 ,$$

where the numerical coefficient was derived by using the F^* dominance of the form factor. Assuming perfect SU_4 symmetry, i.e., $f_+^{D \rightarrow K}(0) = 1$, we obtain

$$|U_{cs}| = .82 \pm .13 ,$$

where the uncertainty quoted represents merely a propagation of the errors in the input quantities and does not reflect any additional theoretical uncertainties.

2 - Independent information on this matrix element can be obtained from the charm production by neutrinos, i.e. from the analysis of $\mu^+\mu^-$ events in the final state. The differential cross section has been given in Equation 2.10 and thus one must separate the two contributions. This can be done because the valence and sea quark distributions have quite different x dependence.

In more detail the procedure is as follows. The $s(x)$ distribution is assumed to be the same as $\bar{s}(x)$ and can be obtained directly from the $\mu^+\mu^-$ events produced by the ν interactions. Because U_{cd} is small, $\bar{u}(x)$ and $\bar{d}(x)$ contribute very little to this process, and in addition they are very similar to $s(x)$ as can be ascertained from single μ production by ν 's at high y . This fact is illustrated in Fig. 6a where the actual $\mu^+\mu^-$ x distribution is compared with the prediction from the single μ data analysis. Finally, the u and d quark distributions can be obtained from the structure functions using the relation

$$x[u(x) + d(x)] = \frac{1}{2}[F_2(x) + xF_3(x) - 2xs(x)] , \quad (2.17)$$

where F_2 and F_3 are derived from the analysis of single muon data.²⁵⁾ As can be seen from Fig. 6b the data can be fit quite well¹⁹⁾ by a linear combination of these two distributions with the result

$$\frac{|U_{cs}|^2 \cdot 2S}{|U_{cd}|^2 \cdot (U + D)} = 1.19 \pm 0.09 \quad (2.18)$$

where $S = \int_0^1 xs(x)dx$ and similarly for U and D . Again, using the results of the single μ experiment, this result can be converted to

$$\frac{|U_{cs}|^2 \cdot 2S}{|U_{cd}|^2 \cdot (\bar{U} + \bar{D})} = 9.3 \pm 1.6 .$$

To go any further we have to make some assumptions. We expect that $2S < (\bar{U} + \bar{D})$ because of the heavier s quark mass. If we take the extreme case of SU_3

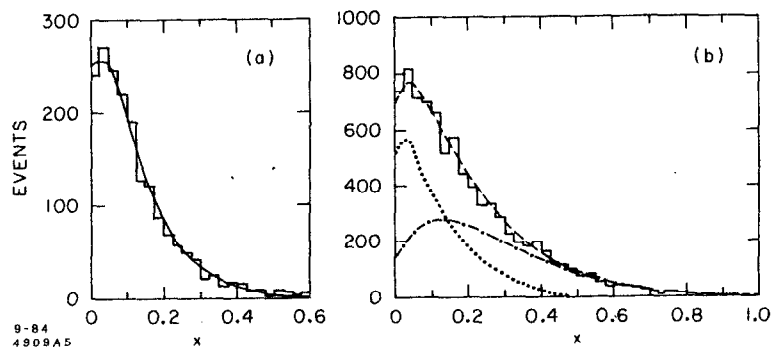


Figure 6 The x distribution for $\mu^+\mu^-$ events from Ref. 19.
 (a) Histogram represents the D data, the curve is the prediction from single μ analysis.
 (b) Histogram represents the ν data; dotted curve is the contribution due to $s(x)$, dash-dot curve due to $u(x) + d(x)$, and the dashed curve the sum of both.

symmetry i.e., $2S = \bar{U} + \bar{D}$ then we obtain

$$|U_{cs}|^2 = (9.3 \pm 1.6)|U_{cd}|^2.$$

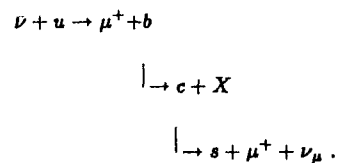
Clearly, this assumption gives a lower limit for U_{cs} . We can plug in the previously derived value of U_{cd} to obtain the inequality

$$|U_{cs}| > 0.59 \text{ at } 90\% \text{ C.L. .}$$

This value is obviously consistent with the result obtained from the charmed meson decay analysis.

e) U_{ub} responsible for the $u \rightarrow b$ or $b \rightarrow u$ transitions.

By far the best limit on this parameter comes from the new information on the b quark lifetimes and the upper limit on $b \rightarrow u$ branching ratio. Before discussing these data, for historical reasons we mention briefly the information that can be extracted from the like sign dimuon data resulting from D interactions. These events could originate (in the quark picture) from:



In the actual calculation,²⁶⁾ it is convenient to compare the rates for $\mu^+\mu^-$ and $\mu^\pm\mu^\pm$ since some of the uncertainties cancel out in that procedure. Threshold factors due to finite c and b quark masses have to be included. The most stringent limit can be obtained by assuming that at least a part of the $\mu^+\mu^+$ rate is due to some background process that also contributes with the same strength to ν interactions, and is responsible there for all of the $\mu^-\mu^-$ events (the cross section

for $\nu\bar{u} \rightarrow \bar{b}\mu^-$ would be much smaller). Under those assumptions one obtains the limit

$$|U_{ub}| < 0.18 \quad (2.19)$$

A much better value is obtained by studying the b decays directly. The important input here is the ratio $\Gamma(b \rightarrow u\nu)/\Gamma(b \rightarrow c\nu)$ which can be obtained from the study of the lepton momentum spectra resulting from the semileptonic b decays. The 4S Υ region is the ideal point to study this question since the B mesons produced are almost at rest and Doppler broadening is relatively small.

This problem was studied by the two collaborations working at CESR and they have obtained the following limits at the 90% C.L.

$$\Gamma(b \rightarrow u\nu)/\Gamma(b \rightarrow c\nu) < 5.5\% \quad \text{CUSB collaboration}^{27)} \quad \text{and}$$

$$\Gamma(b \rightarrow u\nu)/\Gamma(b \rightarrow c\nu) < 4\% \quad \text{CLEO collaboration.}^{28)}$$

There is some model dependance in the extraction of these limits from the data since one has to make some assumptions that affect the exact functional dependance of the curve that is fitted: i.e., spectator quark model or well defined final state mass, Fermi momentum of the b quark, mass of the spectator quark. The end result, however, is only mildly sensitive to these assumptions provided that reasonable values of relevant parameters are taken. The relevant lepton spectra and the fits to different hypotheses are shown in Fig. 7 for the CUSB data and Fig. 8 for the CLEO data.

Taking the more stringent CLEO limit and correcting for phase space effects due to different masses of the u and c quarks we obtain an upper bound

$$|U_{ub}|/|U_{cb}| < 0.14 \quad \text{with 90\% C.L.} \quad (2.20)$$

f) U_{uc} responsible for $c \rightarrow b$ and $b \rightarrow c$ transitions.

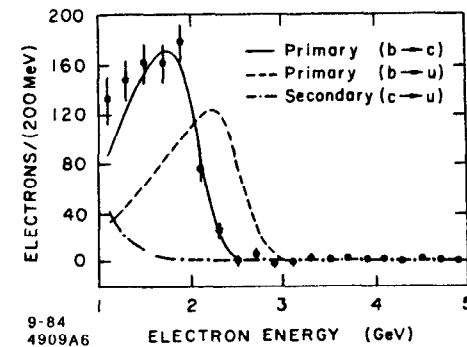


Figure 7 The electron energy spectrum from b decay as obtained by the CUSB collaboration.

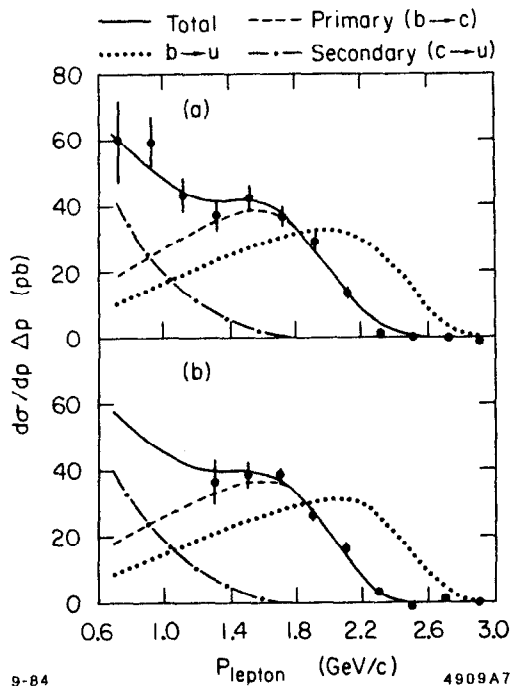


Figure 8 Electron (a) and muon (b) energy spectra from b decay as obtained by the CLEO collaboration. The solid curve represents the calculated spectrum on the assumption of no direct $b \rightarrow ul\nu$ decay.

The lifetime of the b quark can be related to the linear combination of $|U_{cb}|^2$ and $|U_{uc}|^2$. The exact values of the coefficients depend on the quark masses used and on the magnitude of the dynamical enhancement for the non-leptonic modes. We follow the treatment of Gaillard and Maiani²⁹⁾ who derived the relationship:

$$\tau_B = 0.93 \times 10^{-14} / (2.75|U_{cb}|^2 + 7.7|U_{ub}|^2) \text{ sec} \quad (2.21)$$

Note that the ratio of the 2 coefficients, i.e., 0.36 is somewhat different than the ratio of 0.45 used by the CLEO collaboration²⁸⁾ in relating their 4% experimental limit to 0.14 limit on matrix elements previously quoted (using 0.36 would reduce the limit to 0.125).

The b quark lifetime has been shown about a year ago to be surprisingly long³⁰⁾ and the present situation has been summarized by Jaros³¹⁾ at this Institute. The results are tabulated in Table III below.

Table III
Summary of b lifetime results

Collaboration	Value (ps)	Reference
Mark II	$0.85 \pm 0.17 \pm 0.21$	31
MAC	$1.6 \pm 0.4 \pm 0.4$	31
DELCO	$1.16^{+0.37}_{-0.34} \pm 0.23$	32
JADE	$1.8^{+0.5}_{-0.3} \pm 0.35$	33
TASSO	$1.9 \pm 0.4 \pm 0.6$	33

All of these experiments use the impact parameter method^{30,31)} to extract the lifetime value. Thus the systematic errors could be similar and it is probably incorrect to take a weighted average of all the values. For the purpose of the

following discussions we shall take

$$\tau_b = (1.0 \pm 0.3) \times 10^{-12} \text{ sec} .$$

This value yields

$$|U_{cb}| = 0.058 \pm 0.009 \quad (2.22)$$

since the U_{ub} contribution can be neglected here in light of Equation 2.20.

Furthermore, combining this with the Equation 2.20 we also obtain

$$|U_{ub}| < 0.01 \quad 90\% \text{ C.L.} . \quad (2.23)$$

Clearly this limit is much more stringent than the one obtained in 2.19.

g) Other 3 matrix elements.

Clearly no direct experimental information exists at the present time on the other 3 matrix elements that link the t quark to d , s , and b quarks. For completeness, it might be worthwhile to end this discussion by discussing the eventual prospects for measuring these elements.

As will be apparent from the discussion below, we expect the inequality $|U_{tb}| \gg |U_{ts}| \gg |U_{td}|$ based on the extracted values of θ_1, θ_2 , and θ_3 . If the mass of the t quark is in the vicinity of 40 GeV, we would expect an appreciable decay rate³⁴⁾ of the toponium state into $t\bar{b}\ell^- \nu$ and $t\bar{b}\ell^+ \nu$. Since $\Gamma(t\bar{t} \rightarrow e^+e^-)$ can be measured from the height of the toponium peak, the relative branching ratio of $(t\bar{t}) \rightarrow e^+e^-$ vs $t\bar{b}\ell\nu$ can give us the value of $|U_{tb}|^2$. We expect here the usual difficulties associated with measuring an angle by measuring its cosine when $\cos\theta \approx 1$.

In principle the values, or more likely, the limits on the other t quark matrix elements can be obtained by looking at the lepton energy spectra in toponium decays, or bare top decays, in a manner similar to the CESR work on b quarks discussed above. However, because of the high t quark mass, this technique will be rather difficult.

Again, in principle, the top production by neutrinos can yield information on U_{ts} and U_{td} . This method, however, will have to await ν beams of much higher energy than are currently available.

Calculations of the 4 basic parameters: $\theta_1, \theta_2, \theta_3, \delta$.

We can proceed now to the extraction of the 4 basic parameters from the experimental input. We shall use the original Kobayashi-Maskawa parametrization for this purpose. We proceed in several steps:

1 - Since $U_{ud} = C_1$ in K-M parametrization, we obtain directly from Equation 2.5 that

$$S_1 = 0.230 \pm 0.011 . \quad (2.24)$$

2 - We can perform a consistency check using the elements of the first row, which also gives us a value of S_3 . Since

$$U_{us}^2 + U_{ud}^2 = 1 - S_1^2 S_3^2$$

by substituting the experimental values for the expressions on the left hand side of the equation, we obtain

$$S_1 S_3 = \begin{matrix} +.05 \\ .045 \\ -.045 \end{matrix} .$$

Clearly, the unitarity condition is satisfied but the information on S_3 is limited. Dividing by S_1 we obtain

$$S_3 = 0.20 \begin{matrix} +.21 \\ -.20 \end{matrix} . \quad (2.25)$$

This method of obtaining S_3 is much less sensitive than the more direct evaluation discussed below.

3 - Using Eq. 2.23 and definition of U_{cb} we obtain

$$S_1 S_3 < 0.01 \quad 90\% \text{ C.L.}$$

and dividing by S_1 we have

$$S_3 \leq 0.043 \quad 90\% \text{ C.L.} \quad (2.26)$$

4 - From the expression for U_{cb} and Eq. 2.22 we obtain

$$|U_{cb}| = |C_1 C_2 S_3 + S_2 C_3 e^{i\delta}| = 0.058 \pm 0.009$$

which gives us the inequality

$$|S_3 + S_2 e^{i\delta}| \geq 0.058 \pm 0.009 \quad (2.27)$$

The above expression gives us correlated limits on S_2 and S_3 which will occur when $\delta = 0$ and $\delta = \pi$. More precisely, the allowed space for S_2 and S_3 will be a triangular region bounded by the three lines i.e.,

$$\left. \begin{aligned} S_2 &= 0.058 + S_3 & \delta = \pi \text{ case} \\ S_2 &= 0.058 - S_3 & \delta = 0 \text{ case} \\ S_3 &= 0.043 & S_3 \text{ limit} \end{aligned} \right\} \quad (2.28)$$

The intermediate values of δ give well defined contours inside this triangle. These limits as well as contours for other values of δ are displayed in Fig. 9 (adapted from L.-L. Chau and W.-Y. Keung³⁵).

5 - As is apparent from the discussion in the preceding section δ can be determined if both S_2 and S_3 are known. The functional form of the 6 matrix elements discussed above demonstrates that even if the experimental errors were considerably reduced, a unique determination of these two angles is impossible without

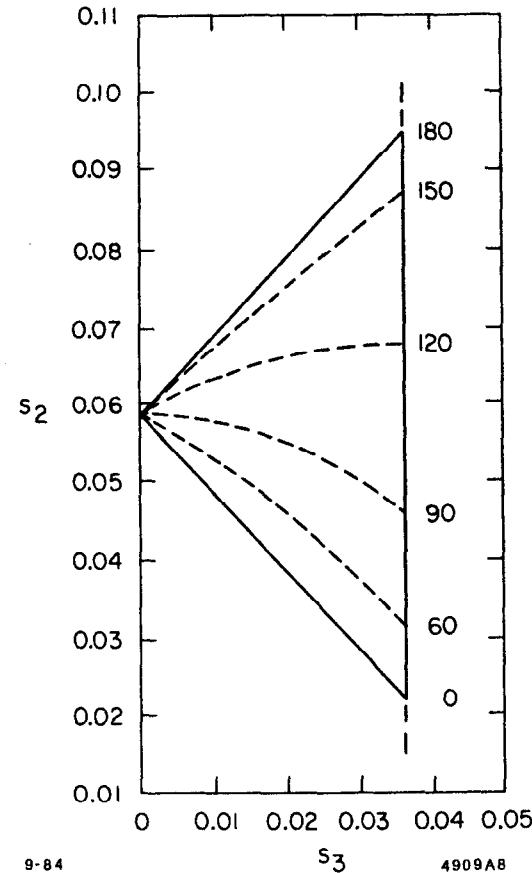


Figure 9 The relationship between S_2 and S_3 values and the value of δ . The allowed S_2 and S_3 values must lie within the triangle bounded by the three solid lines.

additional input. Hence we might discuss briefly which other experiments can provide auxiliary information on these parameters. A full discussion of these questions would take us too far into the theoretical domain; in addition it would unnecessarily duplicate a much more erudite treatment given in the parallel lectures by H. Harari. For completeness, however, we should mention briefly some of the relevant points.

The basic idea is that the off diagonal $K^0 - \bar{K}^0$ mass matrix element is related to several experimentally measurable quantities and that a major (?) contribution to this element is expressible in terms of the K-M matrix elements and hence $\theta_1, \theta_2, \theta_3$, and δ . Some of the quantities related to this matrix element are $\Delta m, K_1 - K_2$ mass difference, CP violation parameter in $K^0 - \bar{K}^0$ system and part of the amplitude for $K^0 \rightarrow \mu^+ \mu^-$. We shall have occasion to return to this point in several instances later on in these lectures. Below we elaborate briefly on the second point.

The off-diagonal $K^0 - \bar{K}^0$ matrix element can be expressed as³⁶⁾:

$$M_{12} = \langle K^0 | H_2 | \bar{K}^0 \rangle + \sum_n \frac{\langle K^0 | H_1 | n \rangle \langle n | H_1 | \bar{K}^0 \rangle}{M_K - E_n} \quad (2.29)$$

where the first part, involving a local $\Delta S = 2$ Hamiltonian can be related to the box diagram shown in Fig. 10, and the second, dispersive part represents a time ordered product of two local $\Delta S = 1$ Hamiltonians. It has been customary to neglect the second part on the grounds that the different contributions enter with both positive and negative signs and hence will cancel out. The contribution of the box diagram,³⁷⁾ M_{12}^{box} , which in this approximation equals M_{12} , can be written as

$$M_{12}^{\text{box}} \propto \sum_{ij}^{u,c,t} \lambda_i \lambda_j A_{ij} K_{12} \quad (2.30)$$

where $\lambda_i = U_{is} U_{id}$ and $i = u, c, t$, and A_{ij} are well defined functions of the quark masses, generally calculated under the assumption that $m_q < m_W$. The matrix

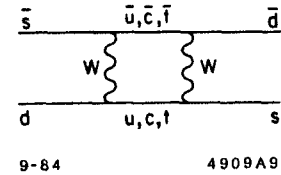


Figure 10 The box diagram used to calculate the short range approximation of $K^0 - \bar{K}^0$ transition amplitude.

element of the $\Delta S = 2$ Hamiltonian is K_{12} . Thus it follows from the above that if

- a) masses of all the quarks are known
- b) one knows how to calculate K_{12} and
- c) the neglect of the long distance contributions is valid,

then the measurement of the quantities expressible in terms of M_{12} will give us information about elements of matrix U. It is important to emphasize these limitations and approximations inherent in these analyses. In practice the approximation (c) is considered to be better for calculations of some parameters than for the others³⁸⁾ (e.g. better for ϵ than for Δm). The uncertainty in K_{12} has been traditionally parametrized by³⁹⁾

$$K_{12} = B(K_{12})_{\text{vac}}$$

where $(K_{12})_{\text{vac}}$ is the vacuum saturation approximation of the matrix element, first used successfully by Gaillard and Lee⁴⁰⁾ in predicting the value of the charmed quark mass and B is usually called the "bag factor" that can be calculated theoretically with a certain degree of reliability.⁴¹⁾ The mass of the top quark has been either used as a parameter in calculating other quantities or has been predicted from other measurements.⁴²⁾

It should be clear from the above that when the top quark mass is known and the value of B is well understood, quite accurate determination of the basic parameters should be possible. Furthermore, different pieces of the experimental input can then be required to be self-consistent. Any discrepancy would be an indication of the new physics that is not contained in the K-M matrix parameters.

Summary.

It is useful to put together all the results on the matrix elements of U. We first compile together the raw experimental data (we quote here magnitudes of

the matrix elements):

$$U = \begin{pmatrix} .9733 \pm .0024 & .225 \pm .005 & < 0.01 \\ .24 \pm .03 & .82 \pm .13 & .058 \pm .009 \\ - & - & - \end{pmatrix}$$

We can obtain more precise values by assuming the unitarity of the U matrix and utilizing the values of θ_1, θ_2 , and θ_3 derived above to calculate the elements of U. This procedure then yields (again magnitudes only):

$$U = \begin{pmatrix} .9733 \pm .0024 & .225 \pm .005 & 0 - 0.01 \\ .225 \pm .006 & .971 \pm .002 & .058 \pm .009 \\ .013 \pm .009 & .058 \pm .009 & .998 \pm .001 \end{pmatrix}$$

3. CP Violation

It has been 20 years almost to the day since the initial observation⁴³⁾ of the CP violation through the decay $K_L^0 \rightarrow \pi^+\pi^-$. The subsequent decade has witnessed a great flurry of activity which established the validity of CP violation interpretation as the explanation of the $K_L^0 \rightarrow 2\pi$ decay, uncovered no evidence of CP violation in any other process, and led to quite accurate measurement of the fundamental CP violation parameters in the $K^0 - \bar{K}^0$ system.⁴⁴⁾

The last few years have seen a revival of the interest in the CP violation question. Part of the stimulation came from the discovery of the heavy quark systems, which could provide a new laboratory for studying these phenomena. More important, however, has been the realization that more precise measurements of the CP violation parameters could shed light on any potential new physics since the prediction of these parameters from the K-M matrix phase δ appears possible.⁴⁵⁾

In this chapter we shall discuss the most recent work on the $K \rightarrow 2\pi$ decays, the prospects for improvement during the next few years, other CP violation experiments planned, and possibilities for observation of CP violation in the heavy quark systems. We shall begin by a brief summary of the formalism needed to describe the $K^0 - \bar{K}^0$ system phenomena.

We define $|K_1^0\rangle$ and $|K_2^0\rangle$ as CP eigenstates, i.e.

$$|K_1^0\rangle = \frac{1}{\sqrt{2}}\{|K^0\rangle + |\bar{K}^0\rangle\} \quad \text{and} \quad |K_2^0\rangle = \frac{1}{\sqrt{2}}\{|K^0\rangle - |\bar{K}^0\rangle\} \quad (3.1)$$

and the actual states observed, $|K_S^0\rangle$ and $|K_L^0\rangle$ as

$$|K_S^0\rangle = \frac{1}{\sqrt{1+|\epsilon|^2}}\{|K_1^0\rangle + \epsilon|K_2^0\rangle\} \quad \text{and} \quad |K_L^0\rangle = \frac{1}{\sqrt{1+|\epsilon|^2}}\{|K_2^0\rangle + \epsilon|K_1^0\rangle\}. \quad (3.2)$$

From the above it is clear that ϵ represents the amount of the "wrong" CP state admixture and thus is a measure of the amount of CP violation in the $K^0 - \bar{K}^0$ system.

One can also have CP violation directly in the $K \rightarrow 2\pi$ decay. This would be the result of a non-zero phase difference between A_0 and A_2 , amplitudes leading to T=0 and T=2 2π states respectively. The standard convention is to define phases in such a way that A_0 is real. Then the direct CP violation parameter ϵ' can be expressed as

$$\epsilon' = \frac{1}{\sqrt{2}} \text{Im} \left(\frac{A_2}{A_0} \right) e^{i(\delta_2 - \delta_0 + \pi/2)} \quad (3.3)$$

where δ_2 and δ_0 are T=2 and T=0 $\pi\pi$ scattering phase shifts that can be measured in independent experiments.

It is also customary to define 2 other amplitudes that are linear combinations of ϵ and ϵ' . These are

$$\eta_{+-} \equiv \frac{A(K_L^0 \rightarrow \pi^+\pi^-)}{A(K_S^0 \rightarrow \pi^+\pi^-)} = \epsilon + \epsilon' \quad \text{and} \quad (3.4)$$

$$\eta_{00} = \frac{A(K_L^0 \rightarrow \pi^0\pi^0)}{A(K_S^0 \rightarrow \pi^0\pi^0)} = \epsilon - 2\epsilon' \quad (3.5)$$

Finally, one should mention the types of experiments that can provide information on these parameters:

- a) The rate of $K_L^0 \rightarrow \pi^+\pi^-$ gives us $|\eta_{+-}|^2$.
- b) The rate of $K_L^0 \rightarrow \pi^0\pi^0$ gives us $|\eta_{00}|^2$.
- c) The charge asymmetry in semileptonic modes is proportional to $\text{Re } \epsilon$.
- d) Interference between coherent K_L^0 and K_S^0 beams decaying into $\pi^+\pi^-$ yields phase of η_{+-} .
- e) Interference between coherent K_L^0 and K_S^0 beams decaying into $\pi^0\pi^0$ yields phase of η_{00} .

The first 4 experiments provide by far the most precise information on the CP violation parameters. One should also mention an important relation that provides a constraint on $\arg \epsilon$, which follows from unitary arguments

$$\tan \arg \epsilon = \frac{2(m_L - m_S)}{\Gamma_S} \quad (3.6)$$

The experiments mentioned above are all consistent⁽⁴⁴⁾ with the superweak model of CP violation⁽⁴⁶⁾ which demands that ϵ' be zero to a very high level of precision. For ϵ they yield the value

$$\epsilon = (2.27 \pm 0.08) \times 10^{-3} e^{i(43.7 \pm 0.2)^\circ}$$

In the last few years there has been a renewed interest in precision measurements of ϵ'/ϵ . Experimentally, this measurement is attractive since due to the relation

$$|\eta_{00}|^2/|\eta_{+-}|^2 = 1 - 6\epsilon'/\epsilon \quad (3.7)$$

which follows immediately from 3.4 and 3.5, a measurement of $|\eta_{00}|^2/|\eta_{+-}|^2$ gives an amplified precision for ϵ'/ϵ by a factor of 6. Furthermore, this measurement

Monte Carlo is lessened.

The basic idea of the Chicago-Saclay experiment is indicated schematically⁴⁶⁾ in Fig. 12. The modes $2\pi^0$ and $\pi^+\pi^-$ are observed at different times, but one does look simultaneously at 2 separate beams, a direct K_L^0 beam and a regenerated K_S^0 beam. The regenerator is moved from one beam to another on a pulse to pulse basis to average out any possible variations in the flux or differences in efficiencies in different areas of the apparatus. An identical regenerator is used for both $\pi^+\pi^-$ and $\pi^0\pi^0$ running. In the $2\pi^0$ mode, one of the γ rays is required to convert in a thin converter which also defines the end of the decay volume. Finally, the rate of decays in both beams is maintained roughly constant by another absorber in the regenerated beam that is located far upstream and moved from one beam to another in phase with the regenerator.

One has to be careful about several potential sources of trouble:

- a) The 2 beams (K_L^0 and K_S^0) have to be well separated so that after reconstruction one can identify unambiguously the source of each 2π event.
- b) The resolutions for the $\pi^0\pi^0$ and $\pi^+\pi^-$ modes are inherently different, both in mass and also in direction. This has the effect that the background that has to be subtracted, both under the K^0 mass peak and under the 0^0 regenerated beam (due to incoherent regeneration) is larger for the $2\pi^0$ mode.
- c) Because of lifetime differences, the longitudinal decay distribution of K_L^0 and K_S^0 will be different. This does introduce some dependance on Monte Carlo calculation of efficiency.

The extent of these potential difficulties and/or the level at which they have been taken care of by the experimenters is illustrated in Figs. 13 - 16. Figure 13 shows that the decays from the two beams are well separated in both the $2\pi^0$ and $\pi^+\pi^-$ modes. Figures 14 and 15 illustrate for 2 typical energies the effects of different resolution for the 2 decay modes. The background is essentially negligible for the $\pi^+\pi^-$ mode; for $2\pi^0$'s it is at the level of few percent both

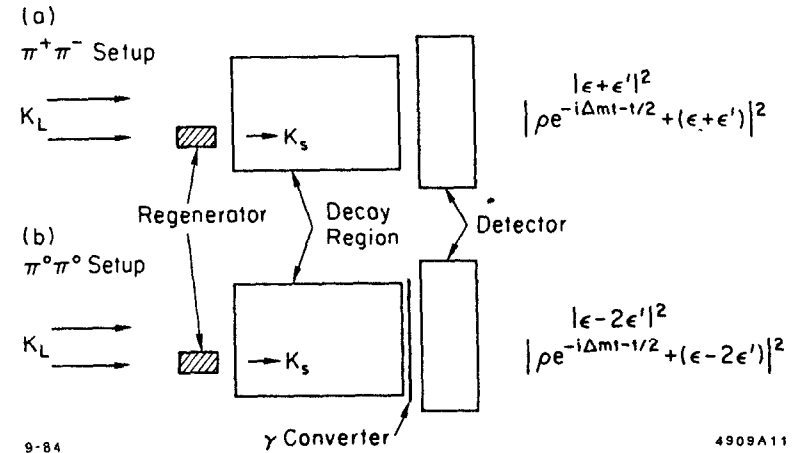
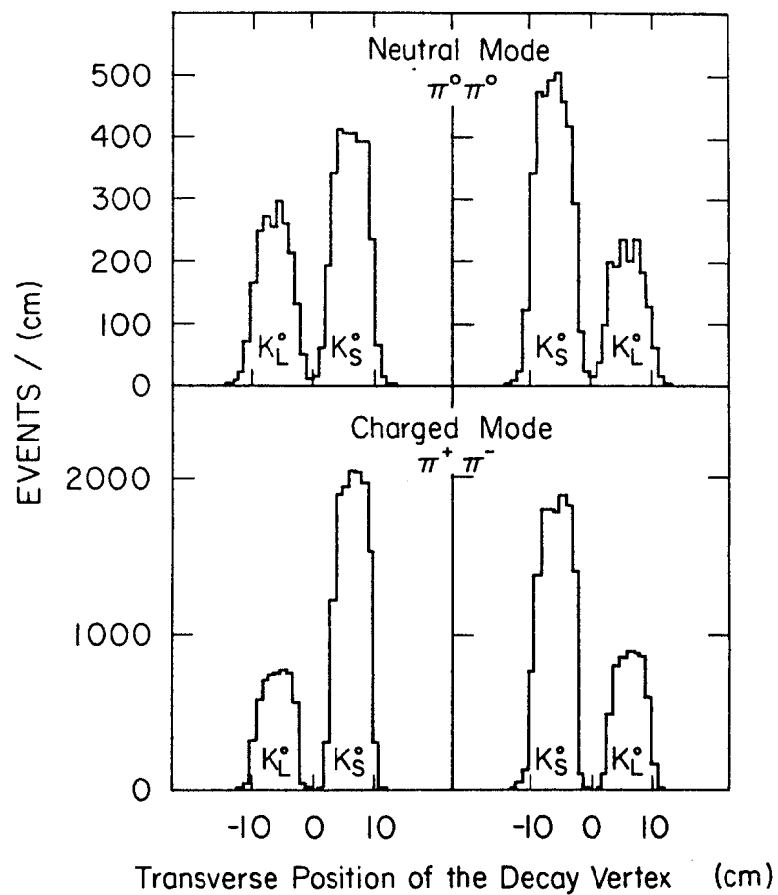


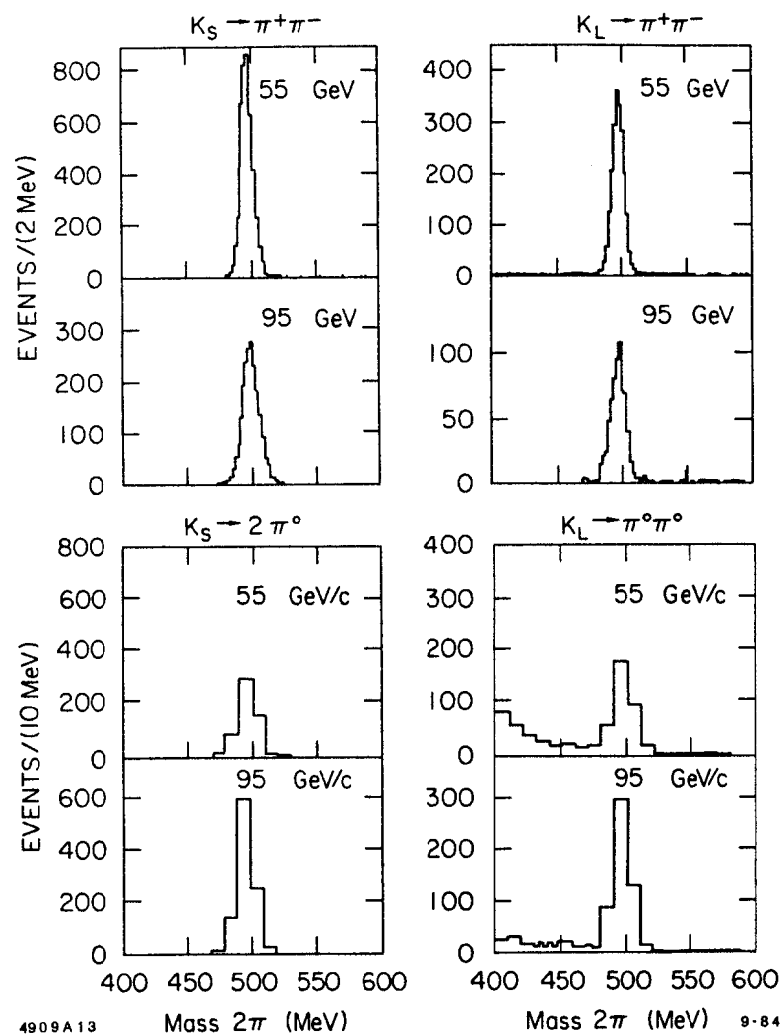
Figure 12 Schematic drawing of the basic idea of the Chicago-Saclay experiment. The amplitudes being measured in each beam are indicated at right.



9-84

4909A12

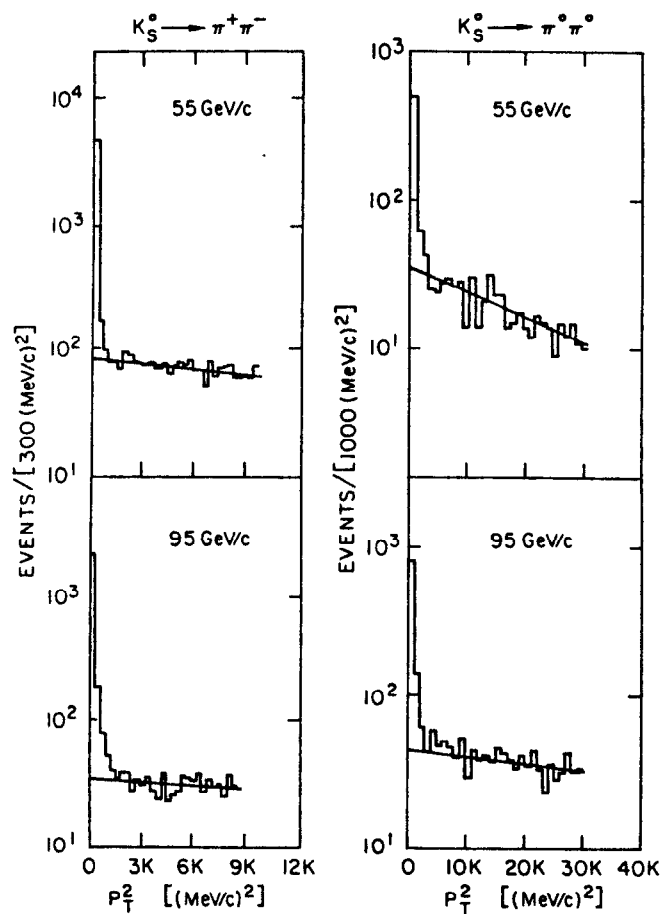
Figure 13 The transverse decay point distribution of the detected events in the Chicago-Saclay experiment.



4909A13

9-84

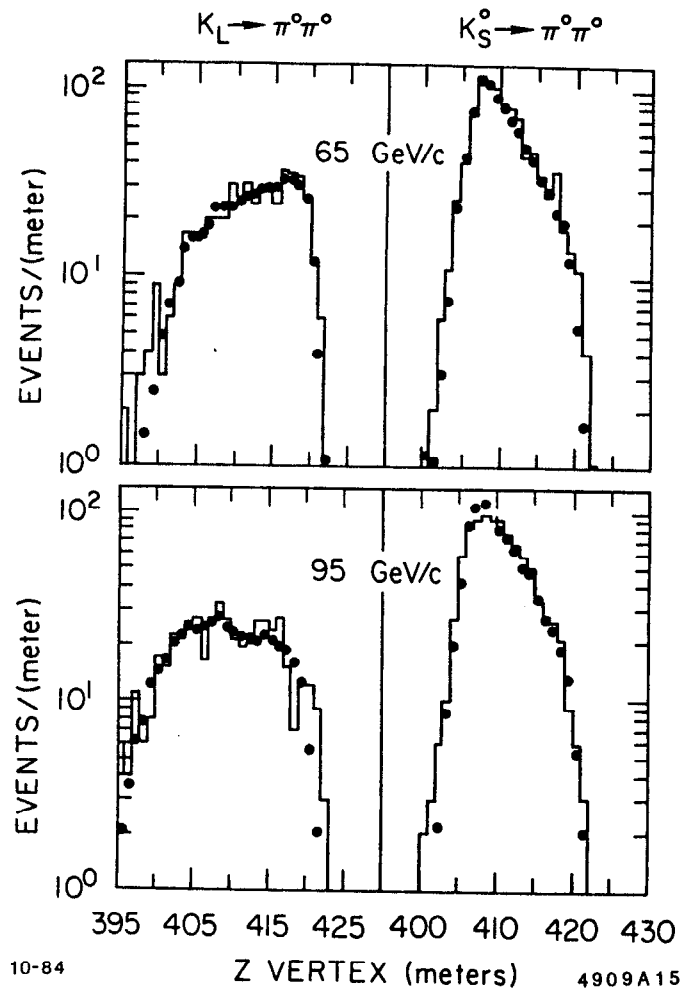
Figure 14 Distribution of the effective mass of the dipion system in the Chicago-Saclay experiment for 2 representative energies.



9-84

4909A14

Figure 15. The P_T^2 distribution of the reconstructed 2π decay events in the regenerator beam for 2 representative energies (from the Chicago-Saclay experiment).



10-84

4909A15

Figure 16 The z distribution of the reconstructed $\pi\pi$ decays of K_L^0 and K_S^0 for 2 representative energies (from the Chicago-Saclay experiment). The solid lines represent the data; the dots the Monte Carlo prediction.

under the mass peak and under the forward coherent regeneration peak. Finally the z dependence of the reconstructed decays and the Monte Carlo prediction is shown in Fig. 16.

In addition, various checks on the systematics have been performed by the group which give one an ability to estimate quantitatively the magnitude of the systematic errors. The final result is

$$\epsilon'/\epsilon = -0.0046 \pm 0.0053(\text{stat}) \pm 0.0024(\text{syst}). \quad (3.9)$$

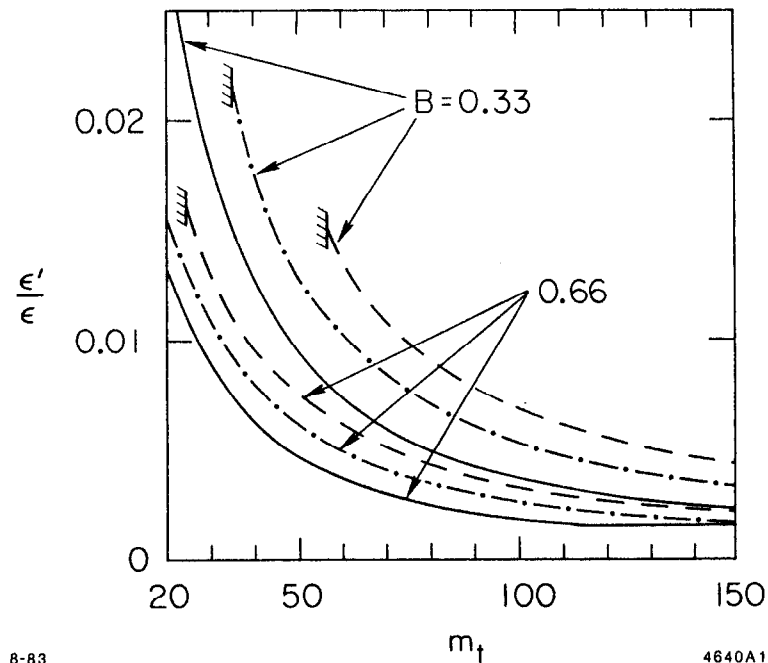
The BNL experiment takes a different approach and collects $\pi^+\pi^-$ and $\pi^0\pi^0$ events simultaneously. The data taking alternates between K_L^0 and K_S^0 , the latter being generated by moving an 80 cm carbon regenerator into the beam. The highly preliminary result quoted by Winstein⁴⁸) at the Dortmund Conference is

$$\epsilon'/\epsilon = -0.0027 \pm 0.0061(\text{stat}). \quad (3.10)$$

The systematic errors are still in the process of being calculated.

These experimental numbers should be compared with the most recent theoretical calculations⁴⁷⁾ of lower bounds on ϵ'/ϵ displayed in Fig. 17. The important point to be made here is that the sign of ϵ'/ϵ is predicted by these calculations and thus there appears to be $\sim 3\sigma$ discrepancy with the experiment.

In light of these results there is a considerable interest in improving the ϵ'/ϵ measurement. There are at present plans for two major new experiments with that goal in mind. The first one, a Chicago-Fermilab-Princeton-Saclay⁵¹⁾ experiment at Fermilab (E731) uses similar techniques as its predecessor, E617. It does, however, take advantage of several improvements, namely better duty cycle at the Tevatron, new and improved beam line, better acceptance, and an improved detector. A data taking rate some 30 times higher than what was achieved previously is anticipated.



8-83

4640A1

Figure 17 Lower bounds on ϵ'/ϵ as calculated by Gilman and Hagelin. Two different values (0.33 and 0.66) of the bag factor B are used, and three different b quark lifetimes: 0.6 psec (solid line), 0.9 psec (dash-dot) and 1.2 psec (dashed line).

A quite different approach has been proposed at CERN⁵²⁾ by the CERN-Pisa-Dortmund-Orsay-Siegen-Edinburgh collaboration. The plan is to take $\pi^+\pi^-$ and $\pi^0\pi^0$ data simultaneously like in the BNL experiment. There are several important and ambitious innovations. The K_S^0 beam is obtained not by regeneration but by targeting the primary proton beam near the detector. This K_S^0 target is movable, the idea being to vary the targeting point along the z direction through the decay volume during the experiment. Thus the K_S^0 and K_L^0 z decay distributions should be very similar. The experiment uses no converter and no magnet and thus achieves very high acceptance. The background to $\pi^+\pi^-$ mode is suppressed by good particle identification, good angular measurements, and use of a hadron calorimeter to measure pion energies. A liquid argon detector is used to measure γ -ray energies and impact points.

These experiments strive for accuracy in the ϵ'/ϵ ratio in the neighborhood of 10^{-3} . The first results should be available in three years.

I would like to summarize next some of the other experiments on CP violation, either performed in the recent past or planned for the near future, that attempt to extend our knowledge of that phenomenon.

a) The CP-nonconserving polarization of μ^+ from the decay $K^+ \rightarrow \pi^0\mu^+\nu$, normal to the decay plane, has been measured recently by the Yale-BNL group.⁵³⁾ For events satisfying $\vec{P}_\mu \cdot \vec{P}_\nu \approx 0$ they obtain a value

$$P = (-3.0 \pm 4.7) \times 10^{-3}.$$

This result, especially when coupled with the earlier companion work on μ polarization from K_L^0 decay,⁵⁴⁾ precludes unusually large contributions to CP violation from the Higgs sector.

b) There are tentative plans at CERN to look for a difference in the branching ratios for $K^0 \rightarrow 2\pi^0$ and $\bar{K}^0 \rightarrow 2\pi^0$, which is allowed if CP invariance is violated. The proposed letter of intent⁵⁵⁾ plans to exploit the fact that at LEAR one has

a very good source of tagged K^0 and \bar{K}^0 decays resulting from the channels

$$\bar{p}p \rightarrow K^+\pi^-\bar{K}^0 \text{ or } K^-\pi^+K^0.$$

The authors propose to look at about 2×10^8 $2\pi^0$ decays which would yield sensitivity on the ϵ'/ϵ ratio of about 3×10^{-3} .

c) A search for CP violation in a new channel is at present under way in a new experiment at Fermilab⁵⁶⁾ by a Rutgers-Wisconsin-Michigan-Minnesota collaboration. The experiment will measure the rate for the decay $K^0 \rightarrow \pi^+\pi^-\pi^0$ as a function of the proper time in the K^0 rest frame. The major contribution to this decay will come from the decay of K_L^0 , but this rate will be modulated at a level of about 10^{-3} by simultaneous presence of a CP violating amplitude due to $K_S^0 \rightarrow \pi^+\pi^-\pi^0$ decay. The interference of this small amplitude will give some time dependence to this rate. If one defines

$$\eta_{+-0} \equiv \frac{A(K_S^0 \rightarrow \pi^+\pi^-\pi^0)}{A(K_L^0 \rightarrow \pi^+\pi^-\pi^0)}$$

one expects a precision on η_{+-0}/ϵ of about 0.25. This can be compared with the present limit of

$$|\frac{\eta_{+-0}}{\epsilon}| < 150.$$

d) A recently approved experiment at BNL, E791, proposes⁵⁷⁾ to look for CP violating mode

$$K_L^0 \rightarrow \pi^0 e^+ e^-.$$

The single γ or Z^0 diagram which contributes to this decay is CP violating and its contribution to the branching ratio can be estimated from the rate of $K^+ \rightarrow \pi^+ e^+ e^-$ decay if the decay occurs solely through the K_1^0 admixture in the K_L^0 state. This rate would involve CP violation in the mass matrix and thus be proportional to $|\epsilon|^2$. The estimated branching ratio from this contribution is 6×10^{-12} .

On the other hand there can also be "direct" CP violation in this decay mode which has been estimated⁵⁸⁾ to generate a branching ratio at the level of 3×10^{-11} . Thus the situation could be quite different here than in the case of $K \rightarrow 2\pi$ decay where the "direct" CP violation amplitude ϵ' is $\lesssim 10^{-2}\epsilon$. The proposed experiment hopes to achieve sensitivity to be able to see the "direct" CP violation.

e) The same experiment⁵⁷⁾ plans also to look for the longitudinal polarization of the μ^+ in the decay

$$K_L^0 \rightarrow \mu^+ \mu^-$$

Two amplitudes can contribute to this process⁵⁹⁾:

$a \equiv {}^1S_0$, which is P and CP conserving, and

$b \equiv {}^3P_0$, which is P and CP violating.

Since a longitudinal polarization of μ^+ violates parity, both of the above amplitudes must be present if that polarization is non-zero, and hence CP must also be violated. In the standard picture, the polarization is expected to vanish at the level of 10^{-3} , so a significant non-zero polarization observed must be evidence of new physics contributing to the process.

The decay rate can be expressed as

$$\Gamma \propto (|a|^2 + \nu^2 |b|^2) \quad (3.11)$$

and the polarization P as

$$P = \frac{2\nu(ba^*)}{|a|^2 + \nu^2 |b|^2}$$

where ν is a phase space factor that is numerically ≈ 0.91 .

The important point here is that considerable theoretical uncertainties exist in calculating the rate for $K_L^0 \rightarrow \mu^+ \mu^-$. The pure weak interaction quark diagrams are not able to account for a significant fraction of the remaining

$K_L^0 \rightarrow \mu^+ \mu^-$ amplitude after the contribution of the 2γ intermediate state is subtracted out.⁶⁰⁾ Thus from the rate measurement alone, one cannot exclude a significant CP violating amplitude b and a polarization close to 100% cannot be ruled out. Furthermore, there is no experimental information at the present time on the polarization in this process.

f) Finally, one should mention the electric dipole moment of the neutron as a potential testing ground of the different models of T violation (and hence also CP violation within the framework of CPT invariance). The present upper limit,⁶¹⁾ quoted as

$$d_n = (0.4 \pm 1.5) \times 10^{-24} e \text{ cm}$$

is already restricting some of the more exotic models of CP violation, but still about 6 orders of magnitude away from the prediction of the standard model.⁶²⁾ Thus even with the experimental improvements anticipated in the near future, the experimental accuracy will not be sufficient to expect a non-zero answer if the K-M phase is the sole source of CP violation.

Heavy quark systems.

We conclude this chapter with a brief discussion of potential CP violation effects in the heavy quark neutral states. The uniqueness of the $K^0 - \bar{K}^0$ system lies in the fact that the only quantum number distinguishing K^0 from its antiparticle is strangeness, i.e., a quantity that is not absolutely conserved. The heavy quark neutral states, $D^0 - \bar{D}^0$, $B^0 - \bar{B}^0$, and $T^0 - \bar{T}^0$ duplicate these conditions insofar as they also differ by a flavor quantum number that is violated by weak interactions. Hence we should ask to what extent the mixing phenomena and mass matrix CP violation, seen in the $K^0 - \bar{K}^0$ system, can be expected to be reproduced also in these heavier neutral systems.

We should first point out that the $B^0 - \bar{B}^0$ system is the most favorable one of the three for the observation of the mixing phenomena.⁶³⁾ The two heavier

quark doublets can be generically represented as

$$\begin{pmatrix} H \\ L \end{pmatrix} \equiv \begin{pmatrix} c \\ s \end{pmatrix} \text{ or } \begin{pmatrix} t \\ b \end{pmatrix} .$$

In general $\Gamma(L) < \Gamma(H)$ because of enhanced phase space for heavy quark (H) decays and even more importantly because the light quark (L) has to decay out of its doublet and hence is Cabibbo suppressed. In addition, if the mass difference is dominated by the box diagrams we would expect

$$\begin{aligned} (\Delta m)_L &\propto M_H^2, \\ (\Delta m)_H &\propto M_L^2 \end{aligned}$$

and hence

$$(\Delta m)_L > (\Delta m)_H .$$

We shall have large mixing if the mass difference is large enough so that the phase between Q_S and Q_L (Q is used as a generic name for a neutral system, e.g. K_S , D_S , etc.) can change appreciably during an average lifetime of that system. Thus $(\Delta m/\Gamma)$ is a measure of the size of that mixing and from the arguments given above we expect that

$$\left(\frac{\Delta m}{\Gamma}\right)_L > \left(\frac{\Delta m}{\Gamma}\right)_H .$$

Hence the K and the B systems should exhibit the greatest mixing effects. Parenthetically, we should mention that experimentally⁶⁴⁾ the $D^0 - \bar{D}^0$ mixing is limited to less than 4%.

In the remainder of this chapter we shall comment very briefly on some of the theoretical calculations regarding the possible mixing and CP violation effects in the $B^0 - \bar{B}^0$ system. One measure of mixing is the parameter r defined as

$$r \equiv \frac{\Gamma(B^0 \rightarrow \ell^+)}{\Gamma(B^0 \rightarrow \ell^-)} .$$

The physical meaning of r is the relative probability that a particle which starts out as a B^0 changes into a \bar{B}^0 , as evidenced by its decay into the "wrong" sign

lepton. It goes without saying, that the leptons discussed above refer to primary leptons only, i.e. do not include secondary leptons from intermediate charm particles. One can show⁶⁵⁾ that r is given by

$$r = \left| \frac{1 - \epsilon_B}{1 + \epsilon_B} \right|^2 \frac{(\Delta m)^2 + \frac{1}{4}(\Delta\Gamma)^2}{2\Gamma^2 + (\Delta m)^2 - 1/4(\Delta\Gamma)^2}$$

where ϵ_B is the ϵ in the B system (parameter characterizing CP violation in the mass matrix) and $\Delta\Gamma \equiv \Gamma_S - \Gamma_L$. Thus we see that r can be non-zero either by virtue of $\Delta m \neq 0$, i.e. mixing due to phase difference or $\Delta\Gamma \neq 0$, which gives rise to mixing by virtue of one linear combination of B's decaying away faster than the other. Both of those terms are appreciable in the $K^0 - \bar{K}^0$ system. For the B's we expect $\Delta m \gg \Delta\Gamma$ since the states that couple to both B^0 and \bar{B}^0 and hence give rise to $\Delta\Gamma$, couple to them relatively weakly⁶⁶⁾ in contrast to the situation with the 2π state in $K^0 - \bar{K}^0$ system.

The CP violation arises if r and \bar{r} are different. In that case the lepton charge asymmetry, which is a true measure of observability of CP violation in the $B^0 - \bar{B}^0$ system is non-zero and is given by

$$A_\ell \equiv \frac{N(\ell^+) - N(\ell^-)}{N(\ell^+) + N(\ell^-)} = \frac{r - \bar{r}}{2 + r + \bar{r}}$$

Clearly mixing is essential if CP violation effects are to be observed.

The $B^0 - \bar{B}^0$ mixing will also lead to like-sign primary dileptons in e^+e^- annihilations. Again we define a mixing parameter R

$$R = \frac{N^{++} + N^{--}}{N^{++} + N^{--} + N^{+-}} = \frac{r + \bar{r}}{r + \bar{r} + r\bar{r} + 1}$$

and a CP violation parameter

$$a \equiv \frac{N^{++} - N^{--}}{N^{++} + N^{--}} = \frac{r - \bar{r}}{r + \bar{r}} .$$

Because the $B^0\bar{B}^0$ pair is produced in a coherent state, the effects of Bose statistics have to be included and the magnitude of R will depend on whether the $B\bar{B}$ is in a relative even or odd angular momentum state.

The magnitude of these parameters have been estimated recently by a number of authors.^{35,47,63,65,66} The calculations can be made for both the $B_d(b\bar{d})$ and $B_s(b\bar{s})$ states and they all depend on the values of the K-M mixing angles and the K-M phase. Using the experimental input on these parameters, one reaches the general conclusion that the mixing parameter can be quite large for B_s but the CP violation parameter a is very small. For B_d , the CP violation parameter is somewhat larger but the mixing effects are correspondingly smaller. The net result is that the CP violation effects due to mass matrix-term will probably be unobservable in the $B - \bar{B}$ system. This situation is summarized in Fig. 18 taken from Ref. 35.

Another possible source of CP violation in the $B^0 - \bar{B}^0$ system would be CP violation in the decay process itself. This could occur in those final states which can be fed by either B^0 or \bar{B}^0 , e.g. $\psi + K_S^0 + \pi$'s. CP violation effects would exhibit itself in a lepton asymmetry in association with such exclusive states. The calculations performed indicate that such asymmetries could be appreciable⁶³ but the statistics will be much more limited because of the requirement to observe an exclusive state.

4. RARE DECAYS

The last several years have seen a renewal of interest in rare decays, more specifically in experimental searches for decays of μ 's, K^+ 's and K_L^0 's which are forbidden in the standard model because they violate one or more conservation laws. These searches are driven in part by the theoretical arguments that new physics might indeed require processes that do not observe these symmetry laws. But they are also fueled by improvement in experimental techniques which make feasible exploration of new domains. In general, most of the ideas for new physics require existence of some new processes and very frequently different schemes make quite different quantitative predictions. Thus experiments on rare decays

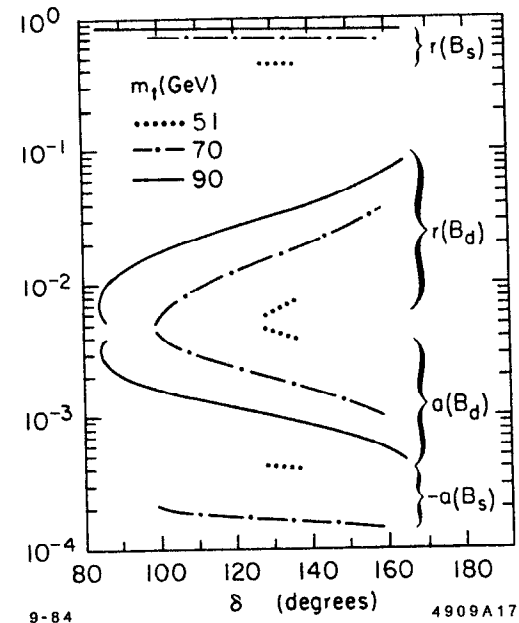


Figure 18 The $B^0 - \bar{B}^0$ mixing parameter r and the CP violation parameter a calculated for B_s and B_d as a function of the top quark mass and the K-M phase δ . The input data uses 1 psec as the b quark lifetime. The allowable range of δ (indicated) is obtained by fitting the ϵ parameter to the box diagram calculation with $B = 0.33$ (from Ref. 35).

are, at least in principle, capable of narrowing down the spectrum of viable new models.

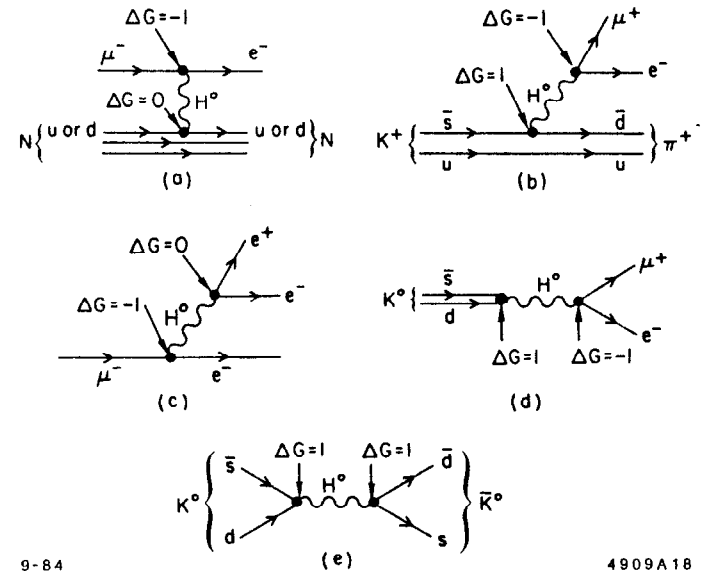
A useful phenomenological classification of different processes has been provided by Cahn and Harari⁶⁷⁾ who utilize the fact that quarks and leptons appear to come in three generations: (u, d, ν_e, e) , (c, s, ν_μ, μ) , and (t, b, ν_τ, τ) each one classified by a generation number G : $G1$ for the first one, $G2$ for the 2nd one, etc. with $G1 - G2 \equiv 1$. In this scheme different diagrams can be classified by their ΔG value. In addition, the reactions can be diagonal or non-diagonal, depending whether the reaction is purely leptonic or hadronic or whether it is mixed. This scheme is illustrated in Fig. 19 which shows the diagrams and Cahn-Harari classification for several processes of interest.

The symmetry violating processes could depend on ΔG and thus different reactions could proceed at quite different rates. But there are other possible relevant factors. Thus if the mediating interaction is of the vector nature, the process $K_L^0 \rightarrow e^\pm \mu^\mp$ will not occur. The same is true for $K^+ \rightarrow \pi^+ e^- \mu^+$ if the relevant interaction is axial. Finally the reaction $K^+ \rightarrow \pi^+ \nu \nu$ is allowed in the standard model with a reasonably well defined rate. But new interactions or phenomena could enhance it or other effects (like large ν_τ mass) could suppress it. The main point of this discussion is that there exists a great wealth of different possibilities in different models and only experiments can resolve these issues.

In contrast to the new K decay experiments that are not scheduled to start taking data for another year or so, the muon rare decay program has been pursued vigorously during the last decade. The main lepton number violating channels that have been studied are:

$$\begin{aligned} \mu^+ &\rightarrow e^+ \gamma, \\ \mu^+ &\rightarrow e^+ e^+ e^-, \\ \mu^- N &\rightarrow e^- N, \\ \text{and } \mu^+ &\rightarrow e^+ \gamma \gamma. \end{aligned}$$

No positive evidence for any of these processes has been found but the great deal



9-84

4909A18

Figure 19 (a) The μ conversion to e by nuclear capture, $\Delta G = -1$;

(b) The $K^+ \rightarrow \pi^+ \mu^+ e^-$ decay, $\Delta G = 0$;

(c) The diagonal process $\mu \rightarrow 3e$, $\Delta G = -1$;

(d) The non-diagonal, $\Delta G = 0$, $K_L^0 \rightarrow \mu e$ decay; and

(e) The $\Delta G = 2$ diagonal interaction which can contribute to $K_L^0 - K_S^0$ mass difference.

of progress that has been accomplished during the last 40 years in this field is illustrated in Fig. 20. The branching ratio for the μ^- capture process is defined as its relative rate with respect to the standard μ^- capture reaction, i.e.,

$$\mu^- N \rightarrow \nu_\mu N'$$

At present there are extensive experimental programs at the three pion and muon factories: LAMPF, SIN, and TRIUMF on the above 3 decay modes and the forbidden conversion process. The present and anticipated branching ratio sensitivity for both μ and K channels is indicated in Fig. 21 where the different processes are explicitly tagged by their ΔG value.

I would like next to discuss several of the planned experimental programs on the rare K decays. They are all scheduled to run at the BNL AGS and can be expected to start yielding results in a period of 1 to 3 years. The first process is the channel

$$K^+ \rightarrow \pi^+ \nu \bar{\nu}$$

or, more correctly, since ν 's are not observed

$$K^+ \rightarrow \pi^+ + \text{nothing visible.}$$

In the standard model, this process is allowed in second order and proceeds via a modified box diagram illustrated in Fig. 22, which effectively turns the \bar{s} quark into the \bar{d} quark. The u quark acts as a spectator. In addition there is an induced Z^0 contribution, also illustrated in Fig. 22. The strength of these contributions can be calculated and the results of the most recent calculations⁴⁷⁾ are shown in Fig. 23 as a function of the top quark mass.

Assuming high experimental sensitivity and a narrowing of the theoretical uncertainties the measurement of this rate could shed light on the number of lepton generations within the framework of the standard picture. The rate for

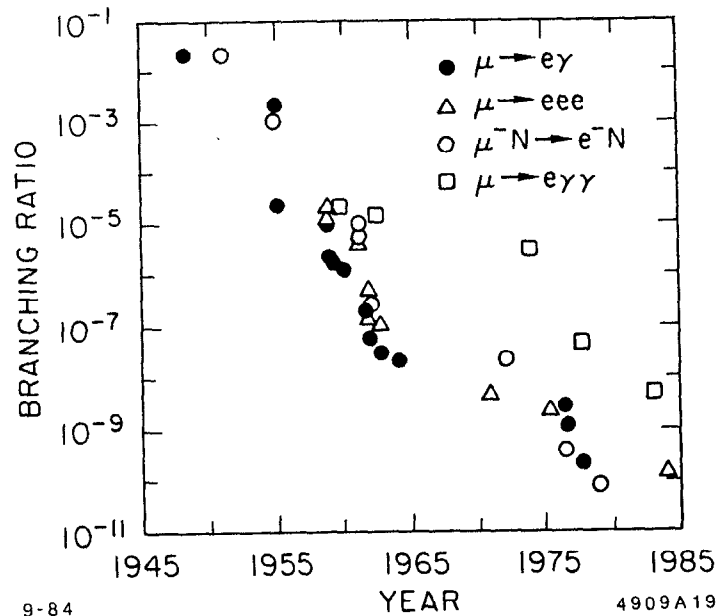


Figure 20 Upper limits for separate lepton number violating processes as a function of time.

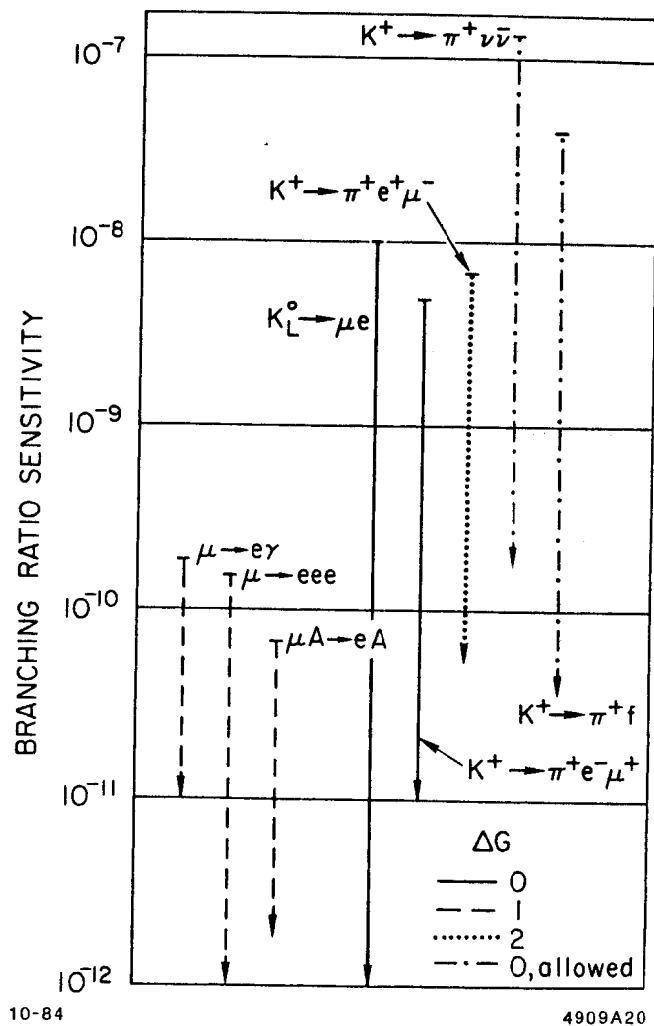


Figure 21 Present and anticipated branching ratio sensitivities for various rare decays.

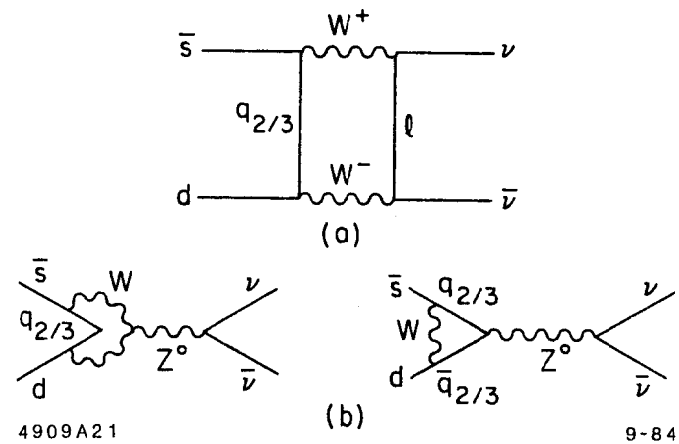


Figure 22 The box diagram contribution to the process $K^+ \rightarrow \pi^+ \nu \bar{\nu}$ (a) as well as some of the diagrams contributing to the induced Z^0 process (b).

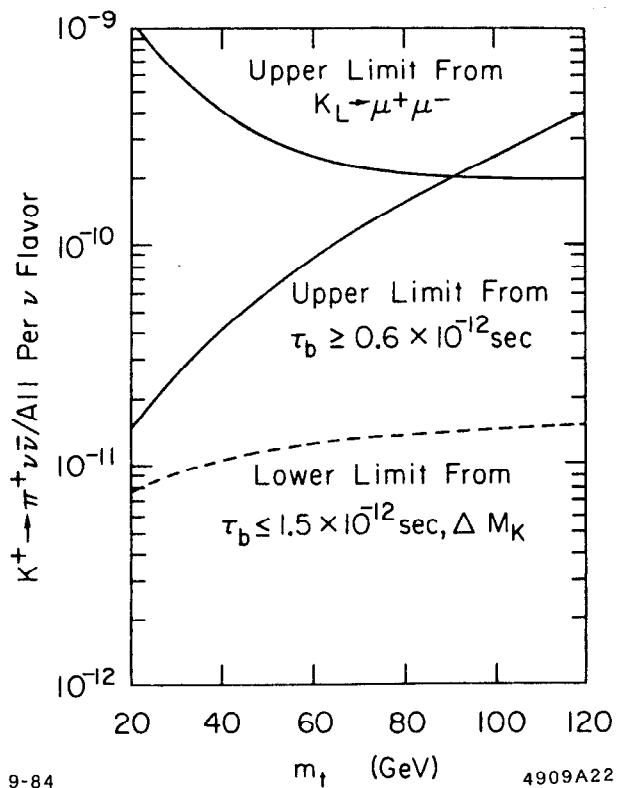


Figure 23 Theoretical limits on the branching ratio $K^+ \rightarrow \pi^+ \nu_i \bar{\nu}_i$ (for each neutrino flavor) as a function of the top quark mass.

each generation has some dependence on the lepton mass(es) in the next generation(s) due to the explicit form of the box diagram,⁶⁸⁾ but this dependence is weak if $m_l \ll m_W$. In addition if the ν_i has an appreciable mass (several MeV or more) the total rate and the π^+ spectrum would be affected.

Probably more interesting is the possibility that there is new physics which contributes to this process. One is the existence of new massless and non-interacting particles, like some of the "nuinos" postulated within the framework of the supersymmetry models. Another new physics possibility is the existence of a new massless Goldstone boson postulated by Wilczek⁶⁹⁾ to explain the lepton and quark masses. This new postulated particle, commonly called familon and denoted by f would exhibit itself in the process under discussion as a decay mode

$$K^+ \rightarrow \pi^+ + f$$

and would result in a peak in π^+ energy spectrum.

Recently an experiment⁷⁰⁾ has been proposed at Brookhaven to investigate this process down to the level of 2×10^{-10} , about three orders of magnitude better than the present upper limit.⁷¹⁾ The main experimental problems center around a clean identification of π^+ and total hermiticity, i.e. ability to detect all the known particles except neutrinos over the full 4π solid angle. The proposed experiment achieves the former, i.e. a good $\pi - \mu$ separation by combining range and curvature information for the momentum measurement and insisting on observation of the full $\pi^+ \rightarrow \mu^+ \rightarrow e^+$ decay chain. The apparatus looks very much like a modest colliding beam detector except that it is totally enclosed by live detectors. The entrance end is capped by a BaF1 scintillator which serves simultaneously to degrade the K^+ beam to a low energy and to detect any decay particles heading in that direction. A fully live and finely segmented target is used to suppress various second order processes that could simulate the decay in question.